UCRL 8260

UNIVERSITY OF CALIFORNIA

Radiation Laboratory

BERKELEY, CALIFORNIA

DISCLAIMER

UCRL-8260

UNIVERSITY OF CALIFORNIA
Radiation Laboratory
Berkeley, California

Contract No. W-7405-eng-48

ANTINUCLEONS

Emilio Segrè

April 1958

Printed for the U. S. Atomic Energy Commission

ANTINUCLEONS[1]

Emilio Segrè

University of California
Berkeley, California

April 1958

Introduction

The idea of "antiparticles", as is well known, originated with Dirac, who in establishing the relativistic equations for the electron noted that besides the solutions corresponding to ordinary electrons there were also "unwanted solutions" corresponding to particles of electronic mass but of charge + e instead of the electronic charge - e.(D2) The discovery of the positron by C. D. Anderson(A10) offered a brilliant experimental confirmation of Dirac's prediction and gave the first example of an "antiparticle."

One could think of applying Dirac's theory of the electron without changes, except in the mass of the particle, to the proton; however, this view is obviously untenable because the magnetic moment of the proton is not one nuclear magneton, nor would it account for the neutron which is clearly related to the proton. Even if such a literal extension of Dirac's theory is impossible, the feature of giving sets of solutions which represent "charge-conjugate" particles is preserved in all theories of elementary particles. In particular the appearance of the anomalous moment of the proton is ascribed to the pion cloud surrounding it and the interaction between pions and nucleons is of the "strong" type for which invariance on charge conjugation is valid(W1). We shall consider only fermions of spin 1/2. For them a particle and its "charged conjugate" are related by the set of properties given in Table 1.

Properties 1-5 inclusive are established by very general arguments and require invariance under the product of charge conjugation C, space reflection P, and time reversal (C P T theorem); they are rigorously true even if invariance under charge conjugation alone is not valid. (See W1 .)

Originally properties 1 - 4 were derived from the principle of invariance under charge conjugation, which can be formulated by saying that a possible physical situation is transformed into another possible physical situation by changing the sign of all electric charges. Since this principle is violated in

---

[1] The survey of the literature pertaining to this review was completed on April 15, 1958.

weak interactions it is important to point out that it is not necessary to establish the properties listed above, but that the weaker requirement expressed by the invariance under the CPT transformation is sufficient.[L1, L2]

Properties 5 and 6 in the nuclear case are a consequence of the conservation of nucleons; the number of antinucleons must be subtracted from the number of nucleons in establishing the nucleon number of a system.

Verification of Dirac's Attributes of the Antiproton

After the discovery of the positron in cosmic rays it was natural to expect that also antinucleons might be found there: indeed prior to 1955 processes in which the energies available were sufficient to produce nucleon-antinucleon pairs occurred only in cosmic rays. Several cosmic ray events[S2, B11, B12, A5] have been observed in cloud chambers and in photographic emulsions which are attributable to antiprotons. In none of them, however, was the evidence obtained at the time of observation sufficient to establish with certainty the identity of the particle involved.

With the advent of accelerators powerful enough to produce antinucleons in the laboratory it became possible to investigate systematically antiprotons and antineutrons, and to identify them beyond any doubt. The first successful investigation was carried on by Chamberlain, Segrè, Wiegand, and Ypsilantis with the Berkeley Bevatron in the fall of 1955.[C8, C9] Charge, mass, and stability against spontaneous decay of the antiproton were the first properties ascertained.

The central problem was to find particles with charge $-e$ and mass equal to that of the proton. This was accomplished by determining the sign and magnitude of the charge, the momentum and velocity of the particle. From the relation

$$p = mc\beta\gamma \qquad (1)$$

the mass was then found. Here p is the momentum, m the rest mass, c the velocity of light, v the velocity of the particle, and $\beta = v/c$, $\gamma = (1 - \beta^2)^{-1/2}$.

The apparatus employed is shown in Fig. 1. The trajectory of the particles fixes their momentum if the charge and the magnetic fields are known. The latter are measured directly and the trajectory is checked by the wire-orbit method: a flexible wire with an electric current i and subject to a mechanical tension T in the magnetic field takes exactly the form of the orbit of

a particle of charge e and momentum p if

$$T/i = p/e \ . \qquad (2)$$

The particles in passing through the scintillation S_1 S_2 S_3 give rise to pulses having the same pulse height as those caused by protons of the same momentum; thus indicating that the magnitude of the charge is e and not 2e or greater. The trajectory determines the sign of the charge as negative and also the momentum p. The measurement of the velocity is the most difficult part of the experiment especially because antiprotons are accompanied by a very heavy background flux of pions mixed with some electrons and muons, in a ratio of the order of 50,000 pions to one antiproton. It is accomplished by measuring the time of flight between scintillators S_1, S_2, and corroborated by the response of the special[C10, W2] Cerenkov Counter C_2 which responds only to particles with $0.75 < \beta < 0.78$. Cerenkov Counter C_1 is in anticoincidence and responds to particles with $\beta > 0.79$. Scintillator S_3 has the purpose of ensuring that the particle is in coincidence and traverses the whole apparatus.

The momentum of a particle passing through the instrument was 1.19 Bev/c. The velocity of an antiproton of this momentum is 0.78c, whereas a meson of the same momentum has v = 0.99c. Their times of flight between S_1 and S_2 were 51 and 40 millimicroseconds respectively. The time of flight and the response of C_2 represent independent velocity measurements, and combined with the other counters as described allow the identification of the particle as an antiproton and a measurement of its mass to 5% accuracy. This apparatus delivers at S_3 certified antiprotons, i.e. it ensures that when the expected electronic signals appear, an antiproton has passed through it and emerged at S_3.

A more luminous version of the apparatus which gives about 80 times as many antiprotons as the one described above is given in reference(A2). At 6.2 Bev this last apparatus gives, as an order of magnitude for practical purposes, one transmitted antiproton of momentum 1.19 Bev/c for every 2.10^{10} protons impinging on a carbon target 6 inches thick. Only about 3% of the antiprotons that enter the apparatus are transmitted. The others are annihilated in the counters, scattered, or otherwise lost.

A spectrograph using repeated time-of-flight measurements, without Cerenkov counters, has been built by Cork and coauthors[C12]; its performance is similar to that of the spectrograph of Ref. A2 but it is better suited for lower momenta where Cerenkov counters are inconvenient.

We shall now discuss how far the properties mentioned in Table I have been verified.

Charge

The sign of the charge is determined by the curvature of the trajectory and its magnitude by the pulse size in the counter experiments and by the grain density in photographic emulsions. Ruling out the possibility of fractional charges, it is - e, identical to the charge of the electron.(C9)

Mass(C9, C3, B3)

The first antiproton experiment gave the mass to an accuracy of five percent. The most precise value of the ratio of the antiproton mass to that of the proton is obtained by the combined use of a measurement of momentum by the wire method and range in a photographic emulsion: a value of 1.010 ± 0.006 has been obtained for the ratio; however, the error reported does not take into account possible systematic errors in the determination of the momentum which, estimated very conservatively, might cause an error in the mass of about 3%.

It is interesting to measure the mass of antiproton by the use of photographic emulsions only, without a separate measurement of the momentum: this has been accomplished by (1) the combination of ionization and residual range and (2) by the combination of ionization and multiple scattering. Ionization was measured by grain density or by measuring the average fraction of a track occupied by silver grains. The emulsions were calibrated directly using protons or deuterons. This work has given a ratio for Method (1) of 1.009 ± 0.027, for Method (2) 0.999 ± 0.043. Again the errors are only statistical. Possible systematic errors might be as high as 3%. (B3)

In conclusion we may sum up by saying that the identity of the mass of the proton and of the antiproton has been verified experimentally to an accuracy of about 2%.

Spin and Magnetic Moment

There are no direct observations of these quantities for the antiproton. A possible method of measurement would be the following: antiprotons generated with a momentum at an angle with the momentum of the particle incident on the target are likely to be polarized. If so the polarization is in a direction perpendicular to the plane defined by the two momenta mentioned above. If they are not polarized at creation, they may be polarized by scattering but this

would increase very appreciably the intensity requirements for an experiment. Assume they are polarized and pass them through a magnetic field H parallel to the momentum. The polarization vector rotates by an angle

$$2\frac{\mu H d}{\hbar c \beta} = a \,, \qquad (3)$$

where μ is the magnetic moment and d the length of the field and $\hbar$ Planck's constant/2π. The angle a is directly measurable by scattering the antiprotons on a target and observing the asymmetry of scattering at different azimuths. All other quantities except μ are easily measurable. The experiment seems feasible with present techniques.(SH3) The spin of the antiproton could also be considered as directly experimentally verified if the magnetic moment would be found, as expected, equal in magnitude to that of the proton: in fact the factor 2 of Eq. 3 is based on a spin 1/2 for the antiproton.

Annihilation

The prediction from Table I is that a nucleon-antinucleon pair, at rest, will annihilate releasing the energy $2mc^2$. No information is given on the form of the energy release; thus, for an electron-positron pair, gamma rays are emitted, whereas for a nucleon-antinucleon pair, pion production is the dominant mode of annihilation. Starting from a nucleon-antinucleon pair we may obtain positive, negative or neutral pions, the latter decaying within 10^{-15} sec. into gamma rays. The charged pions also decay into μ mesons and neutrinos, but the μ mesons decay further into electrons, positrons and neutrinos and in matter the positrons left over annihilate with electrons. Thus, within microseconds the whole rest mass of the system has degraded to forms of energy of rest mass zero with the exception of the case of the antiproton-neutron annihilation in which an electron is left over. Without entering at present in any details concerning the annihilation process, it is clear that in a photographic emulsion where only charged particles leave a track it will not be possible to follow all the annihilation products, but only the charged ones. If, however, at the stopping point of an antiproton we observe an energy release greater than mc^2 we must conclude that the antiproton has annihilated another nucleon, because the visible energy liberated is already greater than the rest energy of the antiproton. The first observation of this phenomenon is reported in Ref. (C_2).

Other methods of observing the annihilation of an antiproton are based on the light emitted either as Cerenkov light or as scintillation light by the charged particles produced directly or indirectly in the annihilation process.

Two typical instruments using Cerenkov light and scintillation light respectively are shown in Figs. 2 and 3. In Fig. 2 the radiator is a large block of glass of refractive index 1.649 for the D lines and radiation length of 2.77 cm. It is observed by a bank of photomultipliers. The light observed is Cerenkov radiation due to the showers produced by neutral pions or produced directly by charged pions.(B10) In Fig. 3(B17) the radiator is a composite sandwich of lead and plastic with an average density of 3.84 g cm^{-3}, an average radiation length of 1.7 cm, and a thickness corresponding to 3 annihilation mean free paths. The total dimensions of the "sandwich" is about 60 × 60 × 60 cm. Both instruments have low resolving power and the annihilation of an antinucleon produces pulses which vary greatly in magnitude, as shown in the figures. Nevertheless an apparatus similar to that of Fig. 2 was used in order to see large annihilation pulses when antiprotons selected by the spectrograph of Ref. (C9) were sent in a piece of glass. The results obtained "were not inconsistent with the expected behavior of antiprotons" but the largest energy release observed as Cerenkov light corresponded only to 0.9 Bev.(B8 , B9)

Production in Pairs

The evidence on the subject comes from the excitation function. The data are still very scanty, but the fact that no antiprotons have been observed at an energy lower than 4.0 Bev for the Bevatron beam is an indication of the production in pairs.(C9)

Thresholds for production in pairs are given in the following table for different processes: (see Table III). We know very little on the production cross sections and their energy dependence (see Sect. "Production") but if the production were not in pairs, process (1) with protons at rest would have for instance a threshold of only 2.35 Bev and the other correspondingly lower. The observed facts do not seem reconcilable with such an hypothesis.

Decay Constant

Antiprotons in a vacuum must be stable. Antineutrons must decay with a mean life of 1040 sec. In the different experiments performed heretofore, the times of flight involved are up to 10^{-7} sec. The decay constant cannot be

much less than the time of flight otherwise no antiprotons would be observed. We have thus lower limits for the mean life of 10^{-7} sec.

Summing up we can say that the properties of Table I are essentially verified.

Nucleonic Properties of the Antiproton

The total isotopic spin $\underline{T}$ of an antinucleon is naturally 1/2 and the formula for the charge

$$\frac{q}{e} = T_3 + \frac{N}{2}$$

where N is the number of nucleons, suggests the assignment of $\underline{T}_3 = -1/2$ to the antiproton and $\underline{T}_3 = 1/2$ to the antineutron. Thus a proton-antiproton pair has $\underline{T}_3 = 0$, but $\underline{T} = 1$, or 0, whereas the proton-antineutron pair or the antiproton-neutron pair have $\underline{T} = 1$.

The intrinsic parity of the antiproton and the antineutron is -1 if that of the proton and neutron is assumed to be + 1.

The justification of this assignment of intrinsic parity is that Dirac's theory predicts for the electron-positron pair in the $^1S_0$ state a 2-quanta annihilation with the polarization of the 2 quanta perpendicular to each other corresponding to a pseudoscalar matrix element $(\underline{e}_1 \cdot \underline{e}_2 \times \underline{p})\, f(p)$ (e_1, e_2 unit vectors indicating the polarization of the quanta, $\underline{p}$ relative momentum). This prediction has been verified experimentally and forces the electron and positron to have opposite parities (see Dl). The same is assumed to hold for the proton-antiproton pair and for the neutron-antineutron pair.

We summarize these properties in Table IV.(M1, N1, W1)

We pass now to the properties which are not predictable on the basis of charge conjugation. They are the most novel ones and their study has barely begun.

We shall divide them in collision cross sections, modes of annihilation, and production.

Collision Cross Sections

Collision of antiprotons on nuclei may lead to elastic scattering, inelastic scattering, annihilation or charge exchange. We shall call the corresponding cross sections σ_e, σ_i, σ_a, σ_c. We consider also the reaction cross

section $\sigma_r = \sigma_i + \sigma_a + \sigma_c$ and the total cross section $\sigma_t = \sigma_r + \sigma_e$.

The experimental data obtained thus far are rather sketchy. We shall treat separately the case of antiproton-nucleon scattering and the case of scattering from complex nuclei.

Experimentally a typical apparatus used (C6) is shown in Fig. 4. A certified antiproton falls on the target which is placed in the slots of C* and, if it is annihilated, it gives Cerenkov light detectable by the photomultipliers. If it crosses the target without annihilation and falls into a cone of semiaperture 14° or 20° it is detected by the circular scintillators. If it is scattered by an angle $\theta \geq 20^\circ$ it is not detected by the scintillators or by the target box. With this apparatus one measures separately σ_a and σ_e (20°), the latter symbol meaning that the elastic scattering has occured with an angle larger than 20°. A "good geometry" arrangement which measures σ_t is shown in Fig. 5.(C13) The data accumulated with this or other methods are shown in Table V and VI. The errors quoted are only statistical. The whole subject is in a very early stage of development and the picture we have thus far is a sketchy one. Moreover there are some features of the experimental results obtained thus far which look suspicious, in particular, the ratio between the scattering and total cross section in hydrogen should be reinvestigated.

It must be noted that most of diffraction scattering is included in the data for beryllium and carbon. Namely, if one computes a $\sigma_e(\theta)$ for $\theta = 0$, including all diffraction, the cross sections are increased by about ten percent. In the data for oxygen, copper, silver, and lead diffraction scattering is practically excluded because $\theta \geq 14^\circ$.

In Table VI the data at 450 Mev have been obtained by investigation of H_2O and D_2O and liquid oxygen and suitable subtraction procedures. The reason for this is that liquid hydrogen has a refractive index too small to be used in a Cerenkov counter to detect annihilation. The data "n" are a simple subtraction of D_2O and H_2O observations. However, a large "Glauber correction"(G5) is necessary in order to take into account the shielding of the neutron by the proton in the deuteron. The extent of this correction is somewhat uncertain.(G5, B7a)

The data on hydrogen give the puzzling result that if we compare the data in good geometry with the data at 450 Mev which are in poor geometry there is no difference in cross section to account for any diffraction scattering. This point needs further experimental investigation.

The salient fact emerging from all these observations is the large cross sections which are obtained for all processes involving antiprotons.(C7)

There have been many theoretical papers on the interpretation of the $\bar{p}$ cross sections.

At present the most promising line of approach to the interpretation of the experimental results seems to be a theory of Ball and Chew (B2, see also (I1) and K2 and Y2) which accounts for the large $p\bar{p}$ and $n\bar{p}$ cross sections. Combination of their nucleon-antinucleon results with the optical model theory will account for the antiproton cross sections in complex nuclei.

The model of Ball and Chew starts from an analogy with p-p scattering. There a model with a hard core of $1/3\ (\hbar/m_\pi c)$ radius and a pion cloud surrounding it is assumed and has been shown by Gartenhaus (G1) and by Signell and Marshak (S3) to give reasonably good agreement with experiment. The nature of the impenetrable core is unaccounted for from a pion theoretical point of view and must be considered as a phenomenological hypothesis whereas the pion cloud can be treated from the point of view of the Yukawa interaction with due refinements. For a $p\bar{p}$ system the impenetrable core is replaced by an absorbing core. This is motivated by theory and justified by the large experimental annihilation cross section. Any antiproton which overlaps even slightly with the core seems to undergo annihilation. This core is surrounded by a meson cloud charge conjugate to the meson cloud surrounding a proton, and the interaction between proton and antiproton can be calculated by the same methods as the proton proton cross section, provided one remembers that the "mesonic charge" of the antiproton and of the proton are opposite. Thus forces derived from the exchange of an even number of pions have the same sign in both cases, but forces derived from the exchange of an odd number of pions have opposite signs in the two cases. This program is carried out by introducing an interaction energy

$$V_c + V_{LS}\,(L\cdot S) + V_T\,S_{12} \tag{5}$$

containing a central, spin-orbit and tensor part. From this one obtains an "equivalent potential" for the eigenstates of the total angular momentum including centrifugal repulsion:

$$V\begin{Bmatrix}\ell=J+1\\ \ell=J-1\end{Bmatrix} = V_C - \frac{3}{2}V_{LS} - V_T + \frac{J(J+1)}{Mr^2} \pm \left[\left(\frac{2J+1}{Mr^2} - \frac{2J+1}{2}V_{LS} - \frac{3V_T}{2J+1}\right)^2 + \frac{36\,J(J+1)}{(2J+1)^2}V_T^{\,2}\right]^{1/2} \tag{6}$$

$$V(\ell=J) = V_C - V_{LS} + 2V_T + \frac{J(J+1)}{Mr^2} \qquad (7)$$

With these potentials one constructs the phase shifts and the penetration coefficients for the partial waves.

The V_C, V_{LS}, V_T are chosen following Gartenhaus[G1] and Signell and Marshak[S3] for the V_{LS} part, but introducing the sign changes required by the change of sign of the interaction energy corresponding to the exchange of one pion. The calculation of Ball and Chew is limited to s, p and d waves, i.e. to energies < 150 Mev but even so it gives very interesting results as shown in Table VII.

The limitation in energy of the present calculations derive from the nonrelativistic approximations made and from the fact that in order to extend the theory to higher energies details near the boundaries of the black zone, which are unknown, become important. The reason for this is that the total potential surrounding the core is composed of a centrifugal part and a part originating from the nuclear forces. The sum of the two forms a barrier which is very wide and flat on the top. This barrier can be treated very adequately with the WKB method and for a given s, or p or d partial wave usually gives either perfect transparency or perfect opaqueness, fairly independently of any reasonable core radius. For higher angular momenta these circumstances do not obtain any more.

The Ball-Chew model can be used to calculate also angular distributions for elastic scattering. These have been computed by Fulco[F6] and show a peak in the forward direction (Fig. 6), very different from the np angular distribution. Experimental results, although not very abundant yet, seem to confirm this feature of the model, which is mainly due to the diffraction scattering connected with the annihilation.[A3]

In the same trend of ideas Koba and Takeda[K2] conclude that at very large energies ($\lambda\!\!\!^{-} \ll a$), $\sigma_a = \sigma_e = \pi a^2$ where a is the radius of the black core, but at lower energies $\sigma_a = \pi (a + \lambda\!\!\!^{-})^2$. Even considering waves of high angular momentum ℓ, the ratio between annihilation and scattering cross sections is limited by the inequality:

$$\sigma_t^{(\ell)} \leq \frac{4}{k^2}(2\ell + 1)\frac{\sigma_e^{(\ell)}}{\sigma_t^{(\ell)}}$$

where $\sigma^{(\ell)}$ is the cross section for the ℓth partial wave. Thus, for a given total cross section, a small ratio of elastic to total cross section can be obtained for large values of ℓ.

It is necessary to check further the prediction of this type of model against experiment, but at this writing it seems to offer great promise of accounting for the facts.

Other calculations on the same subject have been performed by Levy.(L5) In some respects these resemble Ball and Chew's work, but they try to take into account terms in which many pions, not only one or two, are involved. They have been further developed by Gourdin and coauthors.(G11)

Inelastic collisions in which pions are generated, without annihilation of the antinucleon have been considered by Barshay.(B4) He has established selection rules and angular distributions to be expected in such collisions.

In addition to the detailed considerations discussed above there are several relations between elastic cross sections which are independent of detailed models and require only charge independence of nuclear forces, such as:(A9, K3, P1, M1, C1)

$$\frac{d\sigma}{d\omega}(0^\circ)_{p\bar{p}\to n\bar{n}} \geq \left(\frac{k}{4\pi}\right)^2 \left\{\sigma_t(\bar{p}n) - \sigma_t(p\bar{p})\right\}^2 \tag{9}$$

where $\sigma_{p\bar{p}-n\bar{n}}$ means the charge exchange scattering cross section.

$$\sigma_e(p\bar{p}\to p\bar{p}) + \sigma_c(p\bar{p}\to n\bar{n}) \geq \frac{1}{2}\sigma_e(\bar{p}n\to\bar{p}n) \tag{10}$$

$$\sigma_e(p\bar{p}\to p\bar{p}) = \frac{1}{4}\left|a_{if}^{(0)} + a_{if}^{(1)}\right|^2 = \sigma_e(n\bar{n}-n\bar{n}) \tag{11}$$

$$\sigma_c(p\bar{p}\to n\bar{n}) = \frac{1}{4}\left|a_{if}^{(0)} - a_{if}^{(1)}\right|^2$$

$$\sigma_e(\bar{p}n\to\bar{p}n) = \left|a_{if}^{(1)}\right|^2 = \sigma_e(\bar{n}p-\bar{n}p)$$

where $a_{if}^{(1)}$ is the scattering amplitude for T = 1 (triplet) between initial and final states and $a_{if}^{(0)}$ the scattering amplitude for T= 0 (singlet) between initial and final state.

Relations (11) give rise to triangular inequalities:

$$\left|(\sigma(p\bar{p}\to\bar{n}n))^{1/2} - (\sigma(\bar{p}n\to\bar{p}n))^{1/2}\right| \leq (\sigma(p\bar{p}-p\bar{p}))^{1/2} \leq (\sigma(p\bar{p}-nn))^{1/2} + (\sigma(\bar{p}n-\bar{p}n))^{1/2} \tag{12}$$

$$\left|\left\{\sigma(p\bar{p}-n\bar{n})\right\}^{1/2} - \left\{\sigma(p\bar{p}-p\bar{p})\right\}^{1/2}\right| \leq (\sigma(\bar{p}n-\bar{p}n))^{1/2} \leq (\sigma(p\bar{p}-n\bar{n}))^{1/2} + (\sigma(p\bar{p}-p\bar{p}))^{1/2} \tag{13}$$

$$\left|(\sigma(\bar{p}n\text{-}\bar{p}n))^{1/2} - (\sigma(p\bar{p}\text{-}p\bar{p}))^{1/2}\right| \leq (\sigma(p\bar{p}\text{-}n\bar{n}))^{1/2} \leq (\sigma(p\bar{n}\text{-}p\bar{n}))^{1/2} + (\sigma(p\bar{p}\text{-}p\bar{p}))^{1/2} \tag{14}$$

These relations are valid for the differential cross sections as well as for the total cross sections.

At present there are not enough data to evaluate the scattering amplitudes. Pomeranchuk (P1) has pointed out that at high energies we might expect:

$$\left|a_{if}^{(1)} - a_{if}^{(0)}\right| \ll \left|a_{if}^{(1)}\right| \tag{15}$$

$$\left|a_{if}^{(1)} - a_{if}^{(0)}\right| \ll \left|a_{if}^{(0)}\right| \tag{16}$$

This interesting inequality is justified as follows: for each initial state i of definite angular momentum and isotopic spin the scattering matrix to a given final state f is subject to the sum rule

$$\sum_f \left|S_{fi}\right|^2 = 1 \tag{17}$$

The amplitudes for elastic scattering in T = 0 or T = 1 states are $a_{if}^{(0)} = (S_{ii}^{(0)} - 1)$ or $a_{if}^{(1)}$ $(S_{ii}^{(1)} - 1)$ whereas all other amplitudes are S_{fi} for $f \neq i$. At high energies the S_{fi} become small because there are many channels and the sum rule forces each individual S_{fi} to be small, however the elastic scattering amplitudes stay comparable to one because they are equal to $S_{ii} - 1$. As a consequence the amplitudes for elastic scattering $a_{if}^{(1)}$ and $a_{if}^{(0)}$ tend each separately to -1 whereas their difference tends to zero.

Proceeding from the nucleon-nucleon to the nucleon-nucleus processes, an early paper by K. A. Johnson (J1) in lowest order perturbation theory predicted elastic cross sections of the order of 0, 1 geometric. Duerr, M. H. Johnson, and Teller, (J2, D4) on the basis of a special nonlinear theory of nuclear forces, predicted a total cross section of the order of or larger than the geometrical one. This theory seems now untenable, (D3) but it foresaw the experimental results.

The most successful treatments of the nucleon-nucleus interactions have been obtained with the optical model. (N2, G4, A2, N4, M2) In its simplest form one gives to nuclear matter a density distribution using e.g. data from electron scattering. Moreover, nuclear matter has absorption and scattering coefficients which can be connected with the nucleon-antinucleon scattering and annihilation. With such a nuclear model using geometrical optics the scattering and absorption by a nucleus are calculated.

The density distribution used is generally of the form

$$P(r) = \frac{\rho_0}{1 + \exp[(r-R)/a]} . \qquad (18)$$

The parameters have been chosen in (A2) with the following values in ( ):

$$R = r_0 A^{1/3} = 1.08\, A^{1/3} \times 10^{-13} \text{ cm}, \quad a = 0.57 \times 10^{-13} \text{ cm} . \qquad (19)$$

The reaction cross section of the nucleus is then given by a literal application of geometrical optics as

$$\sigma_r = 2\pi \int_0^R (1-e^{-2Ks}) \, bdb = 2\pi \int_0^R (1-e^{-2Ks}) \, sds \qquad (20)$$

where $s^2 = R^2 - b^2$, b is the impact parameter with respect to the center of the nucleus, and the absorption coefficient K is given by

$$K = 3A\bar{\sigma}/4\pi R^3 \qquad (21)$$

with A the mass number and $\bar{\sigma}$ the average total nucleon-antinucleon cross section. A slight refinement of this approach takes into account the finite range of the interaction and nuclear density distribution replacing Ks by $\bar{\sigma} \int \rho(r) ds$. It shows good agreement with experiment.

In a similar fashion one may assume a complex potential (G4)

$$V(r) = \frac{V + iW}{1 + \exp[(R-r)/a]} \qquad (22)$$

and calculate the cross sections. Glassgold has obtained good agreement with the present experimental data taking a potential of this form and $a = 0.65 \times 10^{-13}$ cm, $R = 1.30\, A^{1/3} 10^{-13}$ cm. He has calculated explicitly three cases corresponding to protons and antiprotons as per Table VIII. Calculations with a deep potential well ($\bar{p}$) (L) as required by the hypothesis of Duerr and Teller seem hardly compatible with the experimental results.

Elastic collisions with small deflections give rise to interesting interference phenomena between coulomb and nuclear scattering. These have been observed in photographic emulsions by G. Goldhaber and Sandweiss.(G8) They considered scattering down to a projected angle 1.5° and compared the result with that calculated from a black sphere of radius R and a coulomb field. The radius R was assumed to be $1.64\ A^{1/3}\ 10^{-13}$ cm and corresponds to the annihilation cross section. The agreement with experiment is good. Similar calculations performed with the potentials used by Glassgold also agree with experiment give further support to his choice $\bar{p}$ of parameters as distinct from the choice $\bar{p}'$.

The Annihilation Process

Information concerning the annihilation process is derived mostly from annihilations in photographic emulsions and bubble chambers.(C4, C3, C5, B3, H4, A6, A3 From the technical side the most important development for observing the annihilation in photographic emulsions has been the preparation of beams in which the ratio of antiprotons to undesired particles is increased from the value obtained by a simple selection of momentum and direction from the Bevatron target. We shall call such improved beams "purified." In an impurified beam the ratio of pions to antiprotons is anywhere between 5×10^5 to 5×10^4 depending on the momentum selected. In order to have the $\bar{p}$ tracks easily distinguishable from minimum tracks at the entrance of the stack it is necessary to keep the momentum below about 700 Mev/c. At this momentum the $\pi/\bar{p}$ ratio is about 5×10^5. Increase of the momentum at the entrance is undesirable not only for the reason given above, but also to keep the stack length reasonable.

Efforts to purify the beam were made at an early date by Stork and coauthors(S4) but had meager success because the large absorption cross section for antiprotons, unknown at the time, spoiled the performance of the apparatus.

Later a method was devised by which a beam of selected momentum is passed through beryllium absorbers, out of which the different particles emerge with different momenta. A second momentum selector refocuses the different masses in different spots. The antiprotons are accompanied by a background of about 5×10^4 spurious particles per antiproton which is a gain of a factor 10 in the ratio of antiprotons to background. Moreover, the background particles are almost entirely electrons and mu mesons coming from the pion decay, with only a few percent pions left. They interact only weakly in the plates and are much less disturbing than the original pion background.(C5)

The problem of purification of the beam is encountered also in the use of bubble chambers. An arrangement(A3) has been used in which a purification similar to the one described in (C5) is combined with an electronic command of the flashing of the lights of the bubble chamber, limited to the cases when an antiproton detector signals the entrance of an antiproton in the bubble chamber.

The purification problem has also been attacked by a combination of electric and magnetic fields in a Wien filter. This velocity selector is used in conjunction with momentum analyzers to separate particles of different mass. There are at present two versions of these separators,(M7, C11) which show great promise.

We shall first treat the annihilations in which the antiproton reaches the end of the range and is at rest. Actually with the present photographic technique this means that the kinetic energy of the antiproton is < 10 Mev.

Up to now it has not been possible to recognize effectively the partner in the annihilation in photographic emulsions. A few stars have been observed with no nucleons and an even number of mesic prongs, which could be attributed to $p\bar{p}$ annihilation, but no certain assignment is yet possible. At this writing approximately 220 annihilation stars have been observed and analyzed in photographic emulsions. There are also about 500 stars in propane (A3) and 50 in hydrogen (H4) but their analysis is incomplete yet. One-hundred twenty-seven of the photographic emulsion annihilations occurred at rest and in 93 annihilations occurred in flight. A typical star is shown in Fig. 7. The fragments observed are π mesons, protons, light nuclei such as deuterons and alpha particles, and sometimes, though rarely, K mesons. The maximum number of charged pions in a star thus far observed is 6. The maximum number of charged nuclear particles thus far observed is 16. A distribution of the multiplicity of the charged pions is shown in Fig. 8.

We shall now discuss the experimental information on the visible energy release. The energy available is: $2\,mc^2 + T - B = W$ where T is the kinetic energy in the c.m. and B the small (8 Mev) binding energy of the annihilating nucleon. In order to orient ourselves on the apportioning of W we refer to Fig. 10a and 10b where the fraction of the visible energy going into pions, nucleons or light nuclei is indicated. The few cases in which K mesons have been positively recognized are excluded from this figure.

Looking more in detail one finds a spectrum of pion energy as in Fig. 9 with an average T_π = 182 Mev. For the pions coming to rest in the stack (T_π < 100 Mev) it is also possible to determine the sign and one has found a ratio of π^+ to π^- of 0.36 ± 0.1. (C5) This number is smaller than one would expect on a naive view of the annihilation process which takes into account the n/p ratio in the nuclei and the conservation of isotopic spin. (B3, N3) It is however, not clear whether it is truly representative for all annihilation pions independent of energy.

It is now possible to calculate the average number of pions emitted per annihilation. In the stars without K mesons the observed average pion multiplicity is 2.65 ± 0.12 pions per star. This figure contains a ten percent correction for scanning inefficiency. Assuming charge independence in the annihilation process the number of pions emitted should be 3/2 X (2.65 ± 0.1)

or 4.0 ± 0.15. To this number we must add the pions reabsorbed by the nucleus in which the annihilation occurred. Their energy is manifested by the nuclear fragments and we shall call them "converted pions." The number of converted pions is approximately one, as can be inferred from the fact that the nuclear fragments carry away an energy corresponding to the total energy of a pion. In this estimate we multiply the energy carried away by the visible nuclear fragments, by a factor 2.2 in order to take into account the energy carried by neutrons. By this method we thus arrive to an estimate of the average total number of pions released on annihilation $\overline{N}_{\pi}$, of 5.0 ± 0.1.

We reach a similar result also if we assume that in annihilation the neutral pions have the same energy spectrum as the charged ones. Dividing the total energy available on annihilation by the average energy per pion (observed 322 Mev) we obtain for the number of pions 6.1 ± 0.3. This is to be considered as an upper limit because the pions lose some energy before emerging from the nucleus and a better estimate is obtained by considering for each pion an average energy, at formation of 346 Mev, and also the average energy going into K-mesons. With these corrections $\overline{N}_{\pi} = 5.2 \pm 0.5$.

The great majority of the annihilations in photographic emulsions occur in complex nuclei, and if the annihilation occurred deep inside the nucleus, the escaping pions would traverse the nucleus. The mean free path of pions of an energy of 180 Mev in nuclear matter is estimated to be about 10^{-13} cm, (see e.g. L6) i.e. small compared with the nuclear radius, and the escaping pions would be "converted" into nucleons. The fact that only about one in six of the pions is converted suggests that the annihilation occurs in the very peripheral parts of the nuclei and that most of the resulting pions escape without hitting the nucleus. The large nuclear cross sections are also evidence for this interpretation. Additional support for it comes from the observation that the number of pions "converted" in annihilations of antiprotons in flight is larger by about one than in the annihilations at rest as shown in Figs. 10 and 11. We interpret this effect as due to the deeper penetration of the antiproton in flight into the nucleus, compared to the antiproton at rest. An estimate of the order of magnitude of the mean life of the antiproton in nuclear matter based on these considerations is $\sim 2 \times 10^{-24}$ sec.

No angular correlations of the annihilation pions have been observed thus far, although one could perhaps expect that the nucleus should project a shadow and thus the pions might have the tendency to stay in a hemisphere. However a pion-pion interaction might counterbalance this effect and a clarification of these questions will possibly come from the study of $\bar{p}$ annihilation in hydrogen where the shadow effect is obviously absent.

At the present writing we do not have separated examples of annihilations in different materials except for unanalyzed hydrogen stars.[ ] Some of the other stars are certainly due to complex nuclei because they exhibit nucleons among their fragments, or have a balance of charge different from 0. Some might be due to $p\bar{p}$ annihilation but there is no proof that this is the case. For the stars produced by antiprotons coming to rest there is a selective capture on the part of nuclei different from hydrogen similar to what occurs in the pion capture. The slowing down and capture of antiprotons are discussed theoretically by Bethe and Hamilton.[B7]

It is interesting to consider the possibility of "no prong" stars.[P2] They can be produced by charge exchange, in which the antiproton hits a proton and transforms into a neutron-antineutron pair, or by annihilation in neutral pions only. Both processes are rare and in photographic emulsions represent less than one percent of the terminal events.

On the theoretical side we will dispose briefly of the electromagnetic annihilation:[B] it is similar to the electron positron[D1] annihilation, but has not been observed yet. This is not surprising because it competes very unfavorably against the mesic annihilation. For instance Brown and Peshkin[B13] calculate for the annihilation in flight in the nonrelativistic limit a cross section

$$\sigma = \pi \left(\frac{e^2}{Mc^2}\right)^2 \frac{c}{v} \varkappa(\lambda) \simeq 3.10^{-30}\ c/v\ cm^2 \qquad (23)$$

(The factor $\varkappa(\lambda)$ takes into account the anomalous magnetic moment of the proton λ and has the numerical value 38.5 $\varkappa(0) = 1$), whereas the mesic annihilation cross section is of the order of 10^{-25} cm^2. The mixed annihilation, in gamma rays and mesons, is also very improbable. It has been considered by Michel.[M4]

For the purely mesic annihilation, the most important practically, many authors[A1, G3, G6, A8, B7, L3, A7, 11] have established selection rules

based on the conservation of angular momentum, parity, charge conjugation and isotopic spin. It is possible to analyze the phenomenon with various degrees of detail. As an example we give a table due to Lee and Yang containing the main results: see Tables IX and X. In general a given state can produce different numbers of pions: these numbers, however, are either all even or all odd. Thus, states of spin one produce only even numbers of pions. Selection rules for the emission of K-particles on annihilation have also been considered by Gobel,(G6) and Gatto(G3) and selection rules for the formation of pions in non-annihilating collisions of antiprotons and nuclei have been given by Barshay(B4) as previously mentioned.

Apart from selection rules, repeated attempts have been made to apply Fermi's statistical theory,(F2, B5, S5, B3) to the nucleon-antinucleon annihilation. Using the theory in its simplest form, disregarding conservation of angular momentum and K meson production one obtains the results on the multiplicity of the mesons given in Table XI.

The only arbitrary parameter entering in the calculation is the interaction volume Ω which we express in units $\frac{4}{3}\pi(\hbar/m_\pi c)^3$. One would expect that the volume Ω should be near one, because the interaction range between nucleon and antinucleon is expected to be close to the pion Compton wavelength. The fact that agreement with experiment is obtained instead for Ω close to 10, needs some explanation. One of the most interesting and convincing ideas put forward is due to Koba and Takeda.(K2) They consider the nucleon and antinucleon surrounded by the pion cloud: on annihilation the bare nucleons destroy each other very swiftly, in a time of the order of $\hbar/2mc^2$, giving rise to a meson multiplicity corresponding to a value of Ω near one, but the mesons of the cloud at the moment of annihilation are also released, because the annihilation is a nonadiabatic process, with respect to the periods of the motions of the pions in the cloud which are of the order of $\hbar/E_\pi$ where E_π is the total energy of the pion in the cloud. E_π is estimated to be approximately 350 Mev, from the energy of the annihilation pions. The number of pions in the cloud is estimated to be 1.3 per nucleon or antinucleon. In the annihilation 2.6 pions in average are interpreted as coming from the cloud, the remainder are interpreted as coming from the core annihilations. The core annihilation is treated by the statistical method and using for the volume Ω the value 8/27 corresponding to a radius $(2/3)(\hbar/m_\pi c)$ consistent with other values used in the calculation of cross sections, one obtains 2.2 pions in average from the core annihilation. Thus, the total average multiplicity would be 4.8 to be compared with the

experimental value 5.3 ± 0.6. The hypothesis is developed further in order to obtain not only the average number of pions, but also the distribution among different multiplicities. Moreover, the number of K mesons present in annihilation, which seems smaller than what is predicted, by a straight forward application of the statistical theory agrees better with the Koba-Takeda mechanism. Even if the quantitative agreement with experiment is not perfect, we think that this theory has very considerable merit.

Other authors have stressed the many factors that could affect the annihilation process and are neglected in the statistical theory: such are the pion-pion interaction,(G10) the conservation of angular momentum, the relativistic conservation of the center of gravity(L4) and other selection rules which might tend to suppress certain multiplicities. Indeed it is apparent by considering the sensitiveness of the results to some details of the calculation(B5, B6) that the statistical method cannot be reasonably expected to give quantitative results, as was emphasized by Fermi himself. Adjustment of the parameter Ω might compensate for the crudeness of the approximation.

Intermediate theories such as that of Heisenberg and Landau or modifications of the original Fermi theory introducing a temperature parameter(K4, Y1) have also been tried with improved agreement with the experiment.

Conservation of the I spin combined with the statistical theory gives also predictions for the $\pi^-:\pi^+:\pi^0$ ratio.(N3)

For the cases of low multiplicities Bethe and Hamilton (B7) have made a detailed analysis for capture in light elements, establishing in which states the capture must occur in order to give certain results. They consider also the "nuclear Auger effect". An antiproton is captured in a light nucleus from an atomic orbit and goes into a nuclear orbit releasing energy which is taken up by a nuclear proton which is ejected in a way similar to that of the Auger electrons in x-ray phenomena. It is doubtful that this effect takes place at any appreciable extent because annihilation is probably much faster and takes place before the Auger jump.

An ingenious application of the K multiplicity to measure the spin of the K meson has been made by Sandweiss (S1). In the formulae for the K average multiplicity the statistical weight $(2I_K + 1)$ of the K meson appears and it should be possible to recognize $I_K = 0$ from $I_K = 1$ or more. The average number of K mesons per annihilation is very imperfectly known: the limits are from 1 to 4%. In any way they point to spin 0 for the K-meson.

Production

The collisions in which antiprotons are produced are most probably either of the type: $p + p \rightarrow 3p + \bar{p}$ or $\pi^- + p \rightarrow n + p + \bar{p}$ with all the variations compatible with charge conservation.

In the observations up to now we do not know which of the two processes is most effective.

Experimentally there are only very uncertain data: some measurements have given 38 10^{-30} cm^2 $ster^{-1}$ $(Bev/c)^{-1}$ per copper nucleus for the production in the forward direction at p momentum of 1.2 Bev/c when the target is bombarded with 6.1 Bev protons. (A2)

A few comparisons between different targets show that for the same conditions protons are about as effective as carbon nuclei in producing antiprotons. Considering that the Fermi momentum should also enhance appreciably the production in carbon we must conclude that the nucleons in the carbon nucleons are very ineffective in giving antiprotons. The most natural explanation is the great absorption probability for antiprotons formed inside of the nucleus.

Some calculations which take into account mainly phase space factors in the p-nucleus collision giving rise to antinucleons are reported in ref. (F2) and give $\sigma = 7\ 10^{-26}\ (\epsilon/Mc^2)^{7/2}$. Near threshold the yield of antiprotons should grow as $\epsilon^{7/2}$ if they are formed by pn collisions or as $\epsilon^{9/2}$ if they are formed by pp collision, where ϵ is the energy above threshold in the c.m. system. The extra factor ϵ in this case coming from the necessity of putting one of the outgoing protons in a p state.

Attempts have been made to derive production cross sections near threshold from pion theory: Thorn (T3) has for the reactions:

(1) $p + p \rightarrow \bar{p} + 3p$ a cross section $1.4\ 10^{-29}\ (f^2/4\pi)^4 (\epsilon/m)^{9/2}\ cm^2$

and for (2) $p + n \rightarrow n + 2p + \bar{p}$ a cross section $5.4\ 10^{-29}\ (f^2/4\pi)^4 (\epsilon/m)^{7/2}\ cm^2$

with $f^2/4\pi = 15$. Similar calculations by Fox (F3) and McConnel (M3) are based on an unlikely coupling. Calculations of some features of the production such as energy and angular distribution based only on phase space considerations are to be found in (C3).

More recently Barasenkov and coauthors (B2a) have treated the antinucleon production problem by the statistical method following the idea of Belenky which considers a virtual particle corresponding to a pion and nucleon

in the J = 3/2 T = 3/2 state. They also introduce two Fermi volumes corresponding to the Compton wavelength of the pion or of a K meson and they assume that the volumes to be considered in production differ for various particles. With these hypotheses they compute probabilities of formations of groups of particles and antiparticles at 7 and 10 Bev.

Antineutrons

The most convenient and up to now the only practical way of observing antineutrons is to obtain them from antiprotons by charge exchange and detect them by annihilation. This method of production was indicated immediately after the discovery of the antiproton (C 8) and first demonstrated experimentally by Cork, Lambertson, Piccioni, and Wenzel, (C12) by a counter method in which an antiproton selected from a beam entered an absorber. No charged particle was seen to emerge from it but an annihilation counter of the type described above, showed an annihilation pulse. (Fig. .) Similar experiments are reported in (B17). The phenomenon is graphically shown in Fig. 11 which was taken with a propane bubble chamber. (A3) The antiproton, recognizable by the curvature and grain density of its track comes to a sudden end because it loses its charge to a proton giving rise to a neutron antineutron pair. The antineutron annihilates at the spot so marked giving a typical annihilation star.

It would be highly desirable to be able to detect the antineutrons formed at the target of the Bevatron without having to form first antiprotons and then charge exchanging them. The primary difficulty is the problem of recognizing the antineutrons in the neutral beam emerging from the Bevatron. An ingenious attempt in that direction has been made by Moyer (Y3) and coworkers trying to use antineutrons formed in a reaction:

$$p + n = p + \bar{n} + p + n \qquad (25)$$

in which the 3 nucleons on the right escape combined as a He^3. The reaction is thus a two body reaction with a kinematic such that detection of the He^3 at a certain angle from the incoming beam assures of the presence of the $\bar{n}$ at another angle. Thus a coincidence system, possibly refined by time of flight measurements should locate uniquely the antineutron. Unfortunately also here the probability of the 3 nucleons forming a He^3 nucleus is low. There are not yet definite experimental results.

The charge exchange cross sections have been crudely measured and are indicated in Tables V and VI. Actually what has been measured is $(d\sigma/d\omega)_e$ in the forward direction for $\theta \leq 17^\circ$: for $p\bar{p}$ (B17) obtained 10.9 ± 5.8 mb/ster. Most of the charge exchange will deliver antineutrons in a narrow cone in the forward direction in the laboratory, as in the np charge exchange. Explicit theoretical calculations based on the Ball Chew model are given in (F6).

The charge exchange for heavier nuclei has been also observed and there are indications (B17) that at 500 Mev the charge exchange per nucleus does not vary greatly with A. This means of course that heavy nuclei are very inefficient as charge exchangers. Much of this result may be attributed to the large nucleon antinucleon annihilation cross section which prevents the antiprotons from penetrating the nucleus, and gives rise to a shadow effect from the target. The antineutrons are thus only formed in grazing collisions with the rim of the target. If neutrons are concentrated on the surface of the nucleus, as it is sometimes assumed, we have another reason for depressing charge exchange in heavy nuclei because a $\bar{p}n$ collision may form antineutrons only if negative pions are emitted at the same time, a condition which certainly lowers the cross section.

Antihyperons

There must be also antihyperons and we indicate the threshold for their formation by pion nucleon collision and nucleon nucleon collision (see Table XII) in Bev (B4a).

Baldo-Ceolin and Prowse have reported an event which might be interpreted as a $\bar{\Lambda}_0$ (B1) formed by a 4.5 Bev negative pion on a nucleus.

Table XII

Collision	$\bar{\Lambda}^0$	$\bar{\Sigma}$	$\bar{\Xi}$
nn	7.10	7.43	8.9
πn	4.73	5.24	6.21
most favorable	4.0	4.2	5.1

(Most favorable means a two stage reaction in which a pion is first formed (F) and Fermi energies are also considered.)

Antiprotons in Cosmic Rays

A few possible antiprotons have been found in cosmic rays as mentioned above. (A6 , B11, B12, S2 , T2) A Bevatron event very similar in appearance to the cosmic rays connected stars is reported in (H 1 , H 2).

Amaldi has commented on the frequency of observation of antiprotons in emulsions exposed to cosmic rays. His conclusion is that there are more antiprotons, perhaps by a factor 1000, in cosmic rays than one would expect from an estimate based on extrapolations of the Bevatron data (A4).

Fradkin (F5) has considered the possibility of the presence of antiprotons in the primary cosmic radiation and its effect on the east west asymmetry. He concludes that there are less than 0.17% antiprotons in the primary radiation.

McConnel (M 3) has also estimated the possible abundance of antiprotons in cosmic rays on the basis of meson theory.

Nucleon antinucleon annihilation has been invoked also to explain the high energy Schein events (M 3).

Cosmological Speculations

From the cosmological and astronomical point of view no direct telescopic observations can reveal antimatter. There are some unrealistic schemes, based on the helicity of neutrinos which could in principle do it, but they are completely unfeasible at present.

Burbidge and Hoyle (B 14, B15) have calculated a maximum ratio of antimatter to matter for our galaxy of $\sim 10^{-7}$. They assume an average density of matter of 1 atom cm^{-3} and they show that the presence of antimatter in concentration larger than 10^{-7} median cm^{-3} would give rise to larger kinetic and magnetic energy of the interstellar gas clouds and to cosmic radiation of greater intensity than observed. They calculate also an upper limit for the possible addition of antinucleons to our galaxy and find an upper limit of $9 = 3.10^{-22}$ nucleons cm^{-3} sec^{-1}. These would annihilate with a mean life of 3×10^{14} sec and about 0.1 of the annihilation energy would go into electrons. The upper limit of 9 would obtain if the energy of the turbulent motions of the clouds could be ascribed to these electrons.

The maximum value of 9 could be attained either by capture from an intergalactic medium or by a steady state production in an expanding universe. If the upper limit of the concentration of antimatter (10^{-7} nucleons cm^{-3}) is reached the radio noise of the Crab Nebula, in our galaxy could be accounted for by the annihilation.

Outside of our galaxy the strong radio emission of Cygnus A and Messier 87 could also be due to annihilation processes and Burbidge and Hoyle have pointed out some quantitative coincidences between the energy emitted and what could be expected on annihilation and the fact that one would have a single explanation for the energy of agitation of interstellar clouds in our galaxy, for the radio emission of the Crab Nebula and for the two extragalactic sources Cygnus A and M 87.

The most cosmological speculations both steady state or evolutionary the conservation of nucleons and of leptons would require the simultaneous creation of matter and antimatter in equal amounts. This gives rise to the serious difficulty of a mechanism of separation of matter and antimatter, such as would be given by "antigravity". As an example of a cosmogonic speculation in which antimatter plays a prominent role we shall mention the "universon" of M. Goldhaber (G9).

The question of the gravitational behavior of antimatter can ultimately be resolved only by experiment. If the equivalence principle of general relativity is strictly valid, then the antiparticles are subject to the same gravitational actions as a particle of the same inertial mass. The inertial mass of the antiparticles is equal, also in sign, to that of the corresponding particles as shown by the method used for isolating them, which measures directly e/m, by the conservation of charge which establishes the sign of e, and by the laws of electromagnetism.

Even if we are willing to give up the equivalence principle and wish to speculate on "antigravity," namely, on the hypothesis that an antiparticle in a gravitational field be subject to the force opposite to that experienced by a particle we meet a difficulty in the explanation of the behaviour of a self conjugate particle sugh as the photon which is known to be subject to gravity.

The equlvalence principle could be attributed to the fact that all masses in our universe (earth, sun, our galaxy) are composed or ordinary matter, and that the equivalence principle is violated only to an extent connected to the concentration of antimatter in our universe.(M6) It is clear that all these arguments are extremely speculative and that the existence of antigravity would inflict severe damage on the present structure of physics. Also there is no really strong reason in its favor: on the other hand we repeat that only direct experiment can decide the question.

Acknowledgment

The author is indebted to Drs. G. Chew, G. Goldhaber, H. Steiner, and T. Ypsilantis for reading the manuscript and very useful comments.

Table I

Particle-antiparticle relations		
	Particle	Antiparticle
1) Charge	q	$-q$
2) Mass	m	m
3) Spin	same	
4) Magnetic moment	μ	$-\mu$
5) Mean life	same	
6) Creation	in pairs	
7) Annihilation	in pairs	

Table II

Characteristics of components of the apparatus	
S1, S2	Plastic scintillator counters 2.25 in. diameter by 0.62 in. thick
C1	Cerenkov counter of fluorochemical 0-75, ($C_8F_{16}O$); $\mu D = 1.276$; $\rho = 1.76$ g cm^{-3}. Diameter 3 in.; thickness 2 in.
C2	Cerenkov counter of fused quarts: $\mu D = 1.458$; $\rho = 2.2$ g cm^{-3}. Diameter 2.38 in.; length 2.5 in.
Q1, Q2	Quadrupole focusing magnets: Focal length 119 in.; aperture 4 in.
M1, M2	Deflecting magnets 60 in. long. Aperture 12 in. by 4 in. $B \cong 13,700$ gauss

Table III

Thresholds for nucleon antinucleon pair-production
(Bev kinetic energy in the laboratory)

Process	Target at rest	Target with Fermi Energy of 25 Mev
1) $p + p \rightarrow 3p + \bar{p}$	5.63	4.30
2) $\pi + p \rightarrow 2p + \bar{p}$	3.60	2.85
3) $p + p \rightarrow p + p + \pi$	(T_π=3.60) 4.06[a]	(T_π=2.85) 3.08[a]

p stands for proton or neutron. Naturally electric charge must balance in the reaction.

[a] This is the minimum energy required in order to obtain pions of energy T_π.

Table IV

Spin, parity, I spin of nucleons and antinucleons				
	Proton	Neutron	Antiproton	Antineutron
Spin S	1/2	1/2	1/2	1/2
I spin T	1/2	1/2	1/2	1/2
3d-comp of I spin T3	1/2	-1/2	-1/2	1/2
Parity	+	+	-	-

Table V

Antiproton nucleon cross sections

	T Mev	θ degrees	$\sigma_e(\theta)$	σ_a	σ_c	$\sigma_t(\theta)$	$\sigma_{t\,p}(a,b,c)$	$\sigma_{t\,n}(a,b,c)$	Ref.
	20-230	5	71±25	86±45					G7
H	120	7.5	41^{+10}_{-7}						A3
	133	0	78±12		10^{+8}_{-4}	170±12	28	54	C11
	190	0				135±16	25	45	C13
	197	0	69± 9		11^{+9}_{-5}	156± 9	25	44	C11
	265	0	58± 9		8^{+6}_{-3}	127±12	24	37	C11
	300	0				104±14	23	35	C13
	333	0	53± 5		8^{+6}_{-3}	117± 6	23	34	C11
	450	14	15±12	89± 7	10±6	104± 8	(25)	33	C6
	450	20	17±12			102± 8	(24)	33	C6
	500	0				97± 4	30	35	C13
	700	0				94± 4	45	35	C13
D	450	14		135± 7		174± 8	(54±2)	-	C6
	450	20				172± 8	(45±2)	-	C6
"N"	450	14		46± 8		70± 8	(29±1)		C6
	450	20				70± 8	(21±1)		C6
N	450	14		74		113			C6
	450	20		74		113			C6

[a] From the compilations of

[b] From the compilations of V. P. Djelepov and B. Pontecorvo, Atomiaia Energia 3, 413 (1957).

[c] Numbers in parenthesis directly measured, see C6. $\sigma_t(\theta) = \sigma_a + \sigma_c + \sigma_e(\theta) + \sigma$; for $\theta = 14^\circ$ or larger most of the diffraction scattering is not counted in $\sigma_t(\theta)$.

Table VI

$\bar{p}$-Complex nuclei cross sections (in millibarns)

Target	T (Mev lab)	θ	$\bar{p}$ $\sigma_r(\theta)$	$\bar{p}$ $\sigma_{ann.}$	$\bar{p}$ $\sigma_t(\theta)$	p^+ $\sigma_r(\theta)$	$\sigma_r^{\bar{p}}/\sigma_r^{p^+}$	Ref.
Be	500	2.57			460			C13
	500	0			484± 60			C13
	700	3.65			367			C13
	700	1.90			416			C13
	700	0			425± 50			C13
C	700	25.0	436± 19					C13
	700	2.64			575± 59			C13
	700	0			657± 79			C13
	300	3.55	568±102		618±111			C13
	300	0			655±130			C13
O	457	14	556± 10	453± 9		292± 2		A2
	457	20	517± 10			246± 2		A2
	457	0	590± 12			340± 4	1.74±0.04	A2
Cu	411	14	1240± 82	1040± 61		719± 5		A2
	411	20	1220± 88			640± 4		A2
	411	0	1260± 91			880±10	1.44±0.11	A2
Ag	431	14	1630±170	1500±157		1052± 6		A2
	431	20	1640±183			924± 6		A2
	431	0	1635±188			1170±12	1.39±0.16	A2
Pb	436	14	2850±225	2010±182		1662±36		A2
	436	20	2680±254			1461±10		A2
	436	0	3005±275			1845±40	1.62±0.16	A2
	650			2330±285				C13

Table VII

Theoretical cross sections for nucleon antinucleon interaction in mb at 140 Mev (lab) according to (B 17).

	$p\bar{p}$	$n\bar{p}$	pp	np
Scattering	72	69		
Absorption	96	79	29	60
Charge exchange				

Table VIII

Optical model potentials.(G4) For all three cases the radius parameter is $r_0 = 1.30$ and the diffuseness $a = 0.65\ 10^{-13}$ cm.

Projectile	V (Mev)	W (Mev)
p	- 15	-12.5
$\bar{p}$	- 15	-50
$\bar{p}'$	-528	-50

Table IX

Selection rules for $\bar{p}+p \to m\pi$ or $\bar{n}+n \to m\pi$

State	Spin parity	C	T	G	$2\pi^0$	$\pi^+ + \pi^-$	$3\pi^0$	$\pi^+ + \pi^- + \pi^0$	$4\pi^0$	$\pi^+ + \pi^- + 2\pi^0$	$2\pi^+ + 2\pi^-$	$5\pi^0$	$\pi^+ + \pi^- + 3\pi^0$	$2\pi^+ + 2\pi^- + \pi^0$
$^1S_0$	0^-	+	0	+	×	×	-	-				-	-	-
			1	-	×	×				-	-			
$^2S_1$	1^-	-	0	-	×	-	×		×	-	-	×		
			-	+	×		×	-	×			×	-	-
$^1P_1$	1^+	-	0	-	×	×	×		×	-	-	×		
			1	+	×	×	×	-	×			×	-	-
$^2P_0$	0^+	+	0	+			×	×				-	-	-
			1	-	-	-	×	×	-	-	-			
$^3P_1$	1^+	+	0	+	×	×	-	-	-			-	-	-
			1	-	×	×			-	-	-			
$^3P_3$	2^+	+	0	+			-	-				-	-	-
			1	-	-	-			-	-	-			

× means strictly forbidden, - means forbidden so far as the isotopic spin is a good quantum number.

T = isotopic spin, C = charge conjugation operator, G is a quantum number of special interest in the case of systems of zero nucleons. It corresponds to the operator $C e^{i\pi T_2}$ and for zero nucleons has the eigenvalues ± 1 as indicated in the table.

Table X

Selection rules for $\bar{p}+n \rightarrow m\pi$

State	Spin parity	T	G	$\pi^-+\pi^0$	$2\pi^-+\pi^+$	$\pi^-+2\pi^0$	$2\pi^-+\pi^++n+\pi^0$	$\pi^-+3\pi^0$	$3\pi^-+2\pi^+$	$2\pi^-+n^++2\pi^0$	$\pi^-+4\pi^0$
$^1S_0$	0-	1	-	×			-	-			
$^3S_1$	1-	1	+		-	-			-	-	-
$^1P_2$	1+	1	+	×	-	-			-	-	-
$^3P_0$	0+	1	-	-	×	×	-	-			
$^3P_1$	1+	1	-	×			-	-			
$^3P_2$	2+	1	-	-			-	-			

× means strictly forbidden and - means forbidden so far as the isotopic spin is a good quantum number.

Table XI

Distribution of pion multiplicities, according to Fermi model, for different interaction volumes (production of K mesons neglected)

N_π	Probability for annihilation into N_π pions (%)		
	$\Omega = 1$	$\Omega = 10$	$\Omega = 15$
2	6.4	0.1	0.0
3	33.7	5.6	2.3
4	24.6	21.7	13.4
5	5.0	44.0	40.6
6	0.3	23.7	33.1
7	0.0	5.1	10.6
Average No. of pions $\overline{N}_\pi$	3.3	5.0	5.4

BIBLIOGRAPHY

A1 Afrikian, L. M., Sov. Phys., JETP 4, 135 (1957)

A2 Agnew, L. E., Chamberlain, O., Keller, D., Mermod, R., Rogers, E., Steiner, H., Wiegand, C., Phys. Rev., 108, 1545 (1957)

A3 Agnew, L. E., Elioff, T., Fowler, W. B., Gilly, L., Lander, R., Oswald, L., Powell, W., Segrè, E., Steiner, H., White, H., Wiegand, C., Ypsilantis, T., Phys. Rev. in press

A4 Amaldi, E., CERN Symposium, Vol. 2, page 111, Geneva 1956

A5 Amaldi, E., Castagnoli, C., Cortini, G., Franzinetti, C., Manfredini, A., Nuovo Cimento, 1, 492 (1955)

A6 Amaldi, E., Castagnoli, C., Ferro-Luzzi, M., Franzinetti, C., Manfredini, A., Nuovo Cimento, 10, 5, 1797 (1957)

A7 Amati, D., Vitale, B., Nuovo Cimento, 2, 719 (1955)

A8 Amati, D., Vitale, B., Nuovo Cimento, 3, 1411 (1956)

A9 Amati, D., Vitale, B., Nuovo Cimento, 4, 145 (1956)

A10 Anderson, C. D., Phys. Rev., 43, 491 (1933)

B1 Baldo-Ceolin, M., Prowse, D. J., Bull. Am. Phys. Soc., 3, 163 (1958)

B2 Ball, J. S., Chew, G. F., Phys. Rev., 109, 1385 (1958)

B2a Barasenkov, V. S., Barasev, B. M., Bubelev, E. G., Suppl. Nuovo Cimento, 7, 117 (1958)

B3 Barkas, W. H., Birge, R. W., Chupp, W. W., Ekspong, A. G., Goldhaber, G., Goldhaber, S., Heckman, H. H., Perkins, D. H., Sandweiss, J., Segrè, E., Smith, F. M., Stork, D. H., Van Rossum, L., and Amaldi, E., Baroni, G., Castagnoli, C., Franzinetti, C., Manfredini, A., Phys. Rev., 105, 1037 (1957)

B4 Barshay, S., Phys. Rev., 109, 554 (1958)

B4a Beasley, C. O., Holladay, W., Suppl. Nuovo Cimento, 7, 77 (1958)

B5 Belen'kii, S. Z., Maksimenko, V. N., Nikisov, A. I., Rozenthal, I. L., Usp. Fiz. Nauk, 62, 1 (1957)

B6 Belen'kii, S. Z., Rozenthal, I. S., Sov. Phys., JETP 3, 786 (1956)

B7 Bethe, H., Hamilton, J., Nuovo Cimento, 4, 1 (1956)

B7a Blair, J. S., Phys. Rev. in press

B8 Brabant, J. M., Cork, B., Horowitz, N., Moyer, B. J., Murray, J. J., Wallace, R., Wenzel, W. A., Phys. Rev., 101, 498 (1956)

B9 Brabant, J. M., Cork, B., Horowitz, N., Moyer, B. J., Murray, J. J., Wallace, R., Wenzel, W. A., Phys. Rev., 102, 1622 (1956)

B10 Brabant, J. M., Moyer, B. J., Wallace, R., Rev. of Sc. Inst., 28 421 (1957)

B11 Bridge, H. S., Caldwell, D. O., Pal, Y., Rossi, B., Phys. Rev., 102, 930 (1956)

B12 Bridge, H. S., Courant, H., De Staebler, Jr., H., Rossi, B., Phys. Rev., 95, 1101 (1954)

B13 Brown, L. M., Peshkin, M., Phys. Rev., 103, 751 (1956)

B14 Burbidge, G. R., Hoyle, F., Astron. J., 62, 9 (1957)

B15 Burbidge, G. R., Hoyle, F., Nuovo Cimento, 4, 558 (1956)

B16 Burbidge, G. R., Hoyle, F., Scientific American, April 1958

B17 Button, J., Elioff, T., Segrè, E., Steiner, H., Weingart, R., Wiegand, C., Ypsilantis, T., Phys. Rev., 108, 1557 (1957)

C1 Chamberlain, O., Padova Venezia Conference in press

C2 Chamberlain, O., Chupp, W. W., Ekspong, A. G., Goldhaber, G., Goldhaber, S., Lofgren, E. J., Segrè, E., Wiegand, C., and Amaldi, E., Baroni, G., Castagnoli, C., Franzinetti, C., Manfredini, A., Phys. Rev., 102, 921 (1956)

C3 Chamberlain, O., Chupp, W. W., Goldhaber, G., Segrè, E., Wiegand, C., and Amaldi, E., Baroni, G., Castagnoli, C., Franzinetti, C., Manfredini, A., Nuovo Cimento, 3, 447 (1956)

C4 Chamberlain, O., Chupp, W. W., Goldhaber, G., Segrè, E., Wiegand, C., and Amaldi, E., Baroni, G., Castagnoli, C., Franzinetti, C., Manfredini, A., Phys. Rev., 101, 909 (1956)

C5 Chamberlain, O., Goldhaber, G., Jauneau, L., Kalogeropolous, T., Segrè, E., Silberberg, R., Padova Venezia Conference, Study of the annihilation process in a separated antiproton beam (in press)

C6 Chamberlain, O., Keller, D. V., Mermod, R., Segrè, E., Steiner, H. M., Ypsilantis, T., Phys. Rev., 108, 1553 (1957)

C7 Chamberlain, O., Keller, D. V., Segrè, E., Steiner, H. M., Wiegand, C., Ypsilantis, T., Phys. Rev., 102, 1637 (1956)

C8 Chamberlain, O., Segrè, E., Wiegand, C., Ypsilantis, T., Nature, 177, 11 (1956)

C9 Chamberlain, O., Segrè, E., Wiegand, C., Ypsilantis, T., Phys. Rev., 100, 947 (1955)

C10 Chamberlain, O., Wiegand, C., CERN Symposium Proceedings, Vol. 2 p. 82 Geneva (1956)

C11 Coombs, C., Cork, B., Galbraith, W., Lambertson, G. R., Wenzel, W. A., Post deadline paper, Washington meeting, APS, 1958

C12 Cork, B., Lambertson, G. R., Piccioni, O., Wenzel, W. A., Phys. Rev., 104, 1193 (1956)

C13 Cork, B., Lambertson, G. R., Piccioni, O., Wenzel, W. A., Phys. Rev., 107, 248 (1957)

D1 DeBenedetti, S., Corben, H. C., Annual Rev. Nuclear Sci., 4, 191 (1954)

D2 Dirac, P. A. M., The Principles of Quantum Mechanics (Oxford University Press, 1st Edition, Oxford 1930, 3rd Edition, Oxford 1947)

D3 Duerr, H. P., Phys. Rev., 109, 1347 (1958)

D4 Duerr, H. P., Teller, E., Phys. Rev., 101, 494 (1956)

F1 Feldman, G., Phys. Rev., 95, 1697 (1954)

F2 Fermi, E., Progr. Theor. Phys., 5, 570 (1950)

F3 Fox, D., Phys. Rev., 94, 499 (1954)

F4 Fradkin, M. I., Sov. Phys. Jetp, 2, 87 (1956)

F5 Frye, G. M., Armstrong, A. H., Bull. Am. Phys. Soc., 3, 163 (1958)

F6 Fulco, J. R., Phys. Rev., in press

G1 Gartenhaus, S., Phys. Rev., 107, 291 (1957)

G2 Gatto, R., Nuovo Cimento, 3, 468 (1956)

G3 Gatto, R., Nuovo Cimento, 4, 526 (1956)

G4 Glassgold, A. E., Phys. Rev., 110, 220 , (1958)

G5 Glauber, R. J., Phys. Rev., 100, 242 (1955)

G6 Goebel, C., Phys. Rev., 103, 258 (1956)

G7 Goldhaber, G., Kalogeropolous, T., Silberberg, R., Phys. Rev., in press

G8 Goldhaber, G., Sandweiss, J., Phys. Rev., in press

G9 Goldhaber, M., Science, 124, 218 (1956)

G10 Goto, T., Soryushiron Kenkyu (Jap), 15, 176 (1957)

G11 Gourdin, M., Jancovici, B., Verlet, L., private communication

H1 Hill, R. D., Johansson, Stig, D., Gardner, F. T., Phys. Rev., 101, 907 (1956)

H2 Hill, R. D., Johansson, Stig, D., Gardner, F. T., Phys. Rev., 103, 250 (1956)

H3 Hillman, P., Stafford, G. H., Whitehead, C., Nuovo Cimento, 4, 67 (1956)

H4 Horwitz, N., Miller, D., Murray, J., Tripp, R., Post-deadline paper, Washington Meeting, APS 1958

I1 Iwadare, J., Hatano, S., Prog. Theor. Phys., 15, 185 (1956)

J1 Johnson, K. A., Phys. Rev., 96, 1659 (1954)

J2 Johnson, M. H., Teller, E., Phys. Rev., 98, 783 (1955)

K1 Koba, Z., Progress of Theor. Physics, ... (1958)

K2 Koba, Z., Takeda, G., Progress of Theoretical Physics, 19, 269, (1958)

K3 Kobsarev, I., Schmuschkevic, I., Doklad Akad. Nauk SSSR, 102, 929 (1955)

K4 Kretzschmar, M., ZS f. Physik, ... (1958)

L1 Lee, T. D., Oehme, R., Yang, C. N., Phys. Rev., 106, 340 (1957)

L2 Lee, T. D., Yang, C. N., Elementary particles and weak interactions (Washington, D. C. 1957)

L3 Lee, T. D., Yang, C. N., Nuovo Cimento, 3, 749 (1956)

L4 Lepore, J. V. and Neuman, Phys. Rev., 98, 1484 (1955)

L5 Levy, M., Nuovo Cimento ..... (1958)

L6 Lindenbaum, S., Ann. Rev. Nucl. Sci., 7, 315 (1957)

L7 Lüders, G., Naturwissn, 43, 121 (1956)

M1 Malenka, B. J., Primakoff, H., Phys. Rev., 105, 338 (1957)

M2 McCarthy, I. E., Nucl. Phys., 4, 463 (1957)

M3 McConnell, J., Nucl. Phys., 1, 202 (1956)

M4 Michel, Nuovo Cimento, 10, 319 (1953)

M5 Mitra, A. N., Nucl. Phys., 1, 571 (1956)

M6 Morrison, P., Am. Jour. of Physics, in press

M7 Murray, J. J., Bull. Am. Phys. Soc., 3, 175 (1958)

N1 Nakai, S., Progr. Theor. Phys., 17, 139 (1957)

N2 Nemirovskii, P. E., Doklady Ak. Nauk, USSR, 112, 411 (1957)

N3 Nikishov, A. I., Sov. Phys. Jetp, 3, 976 (1957)

N4 Nozawa, M., Goto, T., Yajima, N., Nakashima, R., Progr. Theor. Phys., 17, 504 (1957)

P1 Pomeranchuk, I. Ja., Sov. Phys. Jept., 3, 306 (1956), Zu Eksper. Teor. Fiz., 30, 423 (1956)

P2 Pontecorvo, B., Sov. Phys. Jept., 3, 966 (1957)

S1 Sandweiss, J., Thesis, AEC, Rad. Lab., W-7405-eng-48, (1956), On the Spin of K Mesons from the Analysis of Antiproton Annihilations in Nuclear Emulsions

S1a Segrè, E., Padova Venezia Conference, in press

S2 Shrinkantia, G. S., Nuovo Cimento, 12, 807 (1954)

S3 Signell, P. S., Marshak, R. E., Phys. Rev., 109, 1229 (1958)

S4 Stork, D. H., Birge, R. W., Haddock, R. P., Kerth, L. T., Sandweiss, J., Whitehead, M. N., Phys. Rev., 105, 729 (1957)

S5 Sudarshan, G., Phys. Rev., 103, 777 (1956). This paper contains numerical errors

T1 Tarasov, A., Sov. Phys. Jetp., 3, 636 (1956)

T2 Teucher, M., Winzeler, H., Lahimann, E., Nuovo Cimento, 3, 228 (1956)

T3 Torn, R. N., Phys. Rev., 94, 501 (1954)

W1 Wick, G. C., Ann. Rev. of Nucl. Sci., 8, ... (1958)

W2 Wiegand, C., Transactions of the IRE, Proceedings of the 6th Scintillation Counter Symposium, Washington, D. C., 1958

Y1 Yajima, N., Kobayakawa, K., Progr. Theo. Phys., 19, 192 (1958)

Y2 Yamaguchi, Y., Progr. Teor. Phys., 17, 612 (1957)

Y3 Youtz, B., Am. Jour. of Physics, 26, 202 (1958)

FIGURE CAPTIONS

Fig. 1. Original mass spectrograph of Chamberlain, Segrè, Wiegand, and Ypsilantis (C9). For characteristics of components see Table II.

Fig. 2. Schematic arrangement of the spectrometer showing the glass, phototubes, and magnetic field, as well as the anticoincidence counter, lead, and coincidence counters. These two scintillation counters insure that the electron showers, which are pulse height analyzed, start in the 0.25-inch lead converter and thus are centered in the glass as well as all start at its front surface.

Fig. 3a. Element of the annihilation detector.

Fig. 3b. Assembly of the annihilation detector.

Fig. 4. Arrangement for measuring annihilation cross section and $\sigma_t(\theta)$ (from C6).

Fig. 5. Good geometry arrangement for measuring total $\bar{p}$-p cross sections (from C13).

Fig. 6. Angular distribution in $p\bar{p}$ scattering. Theoretical curve of F(6) at 140 Mev. Experimental results of (A3).

Fig. 7. An annihilation star (C6) showing the particles as numbered

No.	1	2	3	4	5	6	7	8
Identity	p?	π^-	π?	p	π^+	H^3(?)	π^-	π
T (Mev)	10	43	175	70	30	82	34	125

Total visible energy 1300 Mev. Total energy release > 1400 Mev.

Fig. 8. Number of charged pions per annihilation star in photographic emulsions. Stars in flight give $\langle N_{\pi^\pm} \rangle = 2.29 \pm 0.016$. Stars at rest give $\langle N_{\pi^\pm} \rangle = 2.50 \pm 0.15$. These numbers are not corrected for scanning inefficiency, (see text) from C5.

Fig. 9. Distribution of the kinetic energy of charged pions emitted in annihilation stars in nuclear emulsions. The curves marked $N_\pi = 4$ etc. are energy distributions obtained by the statistical method on the hypothesis that the average number of pions emitted is 4, 5 etc. Note that the experimental results agree with an average number of pions emitted comprised between 6 and 7. (From C5.)

Fig. 10. Visible energy in annihilation stars in photographic emulsions. Evaporation protons have T < 30 Mev by definition. Knock on protons have T > 30 Mev by definition. W is the total energy of the antiproton at annihilation. Note that stars in flight compared with stars at rest have a larger fraction of the energy in nucleons.

Fig. 11. An antiproton enters a propane bubble chamber, and at the point marked with the arrow undergoes charge exchange. The antineutron originates the annihilation star. ρ of propane 0.42 gr cm^{-3}. Real distance between charge exchange and origin of star 9.5 cm. $T_{\bar{p}}$ at charge exchange ~ 50 Mev. The visible energy in the star is $\geq$ 1500 Mev.

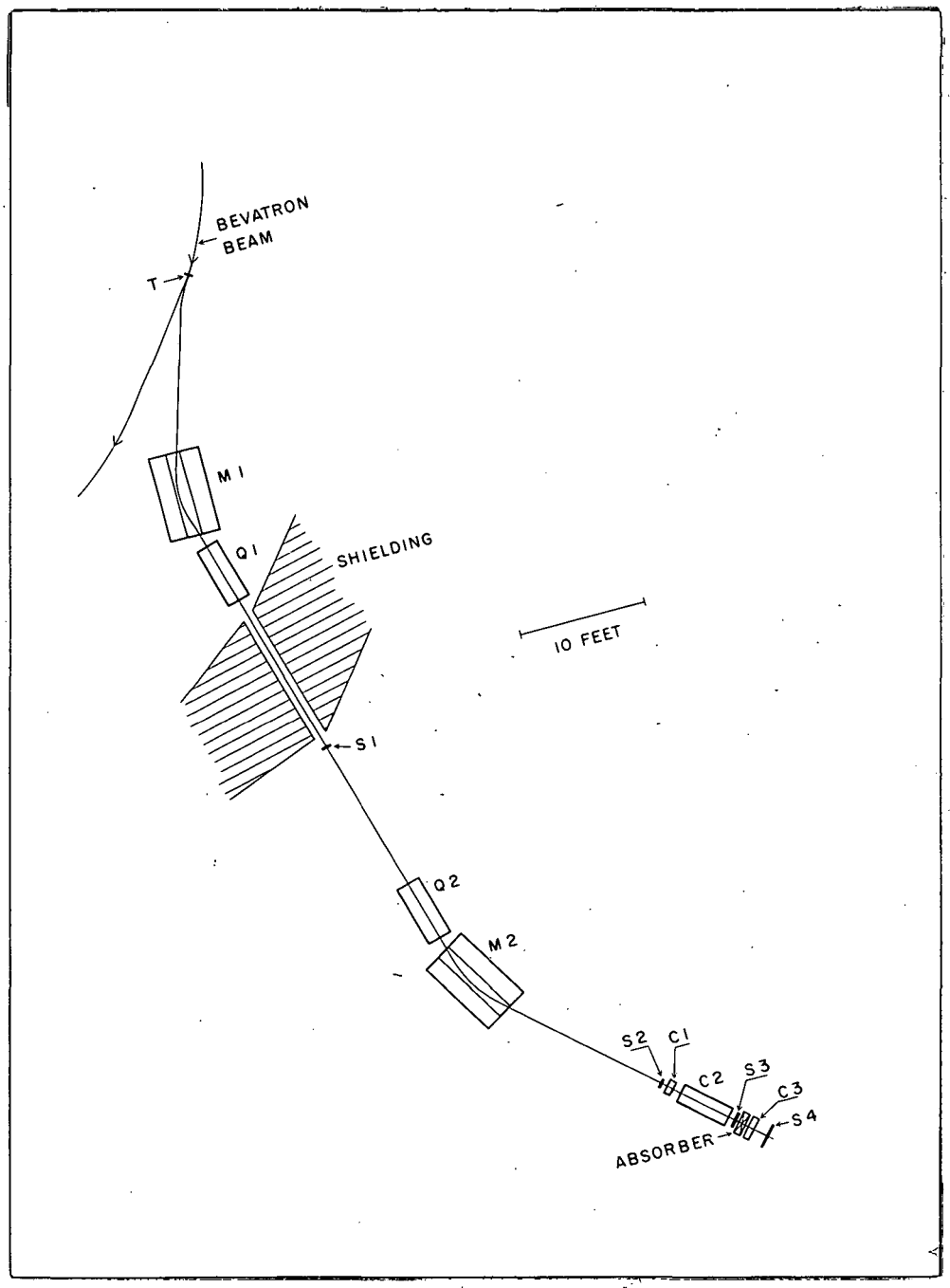
BEVATRON
BEAM
T
M 1
Q 1
SHIELDING
10 FEET
S 1
Q 2
M 2
S2
C1
C2
S3
C3
S4
ABSORBER

Fig. 1

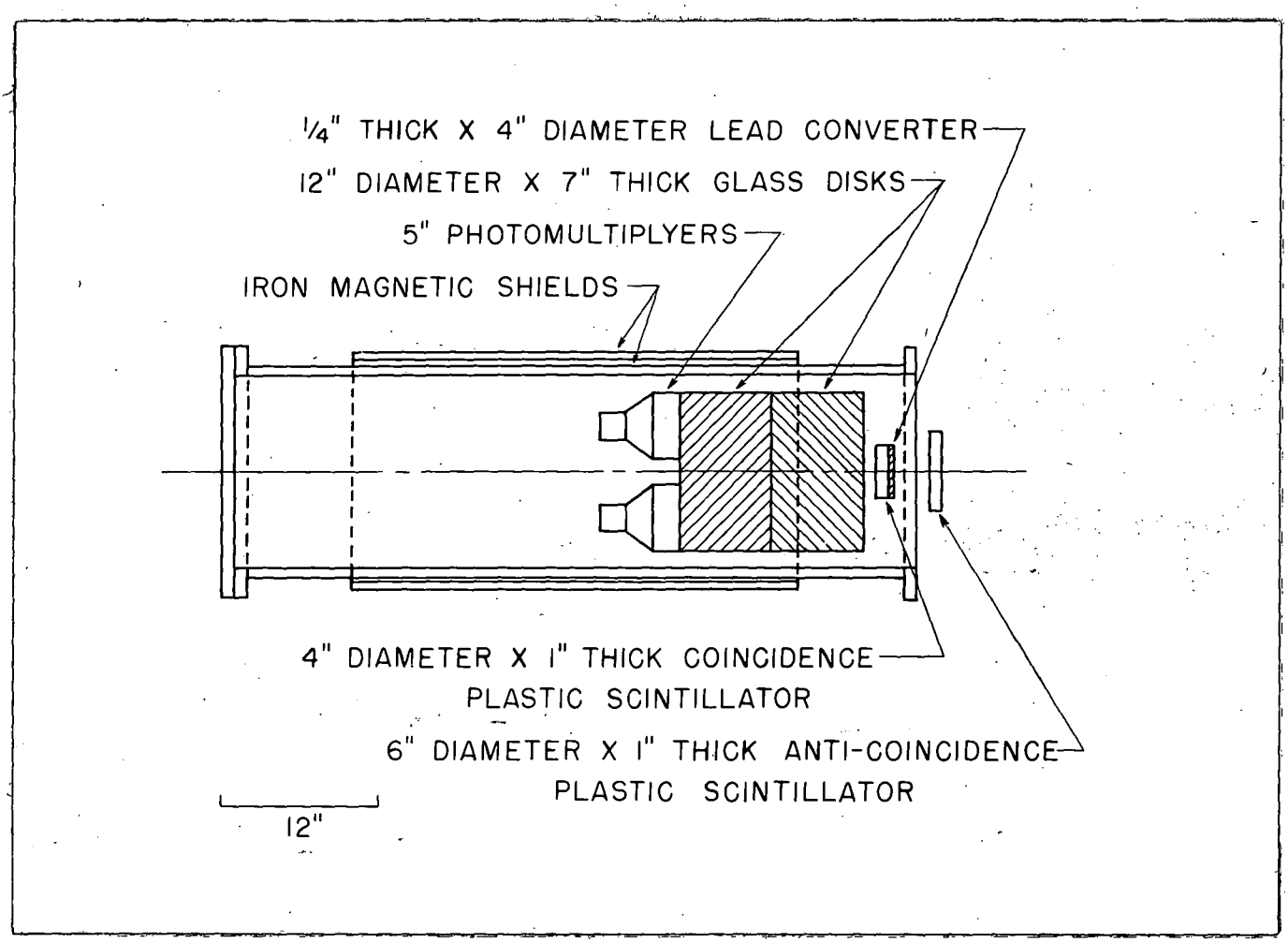
1/4" THICK X 4" DIAMETER LEAD CONVERTER
12" DIAMETER X 7" THICK GLASS DISKS
5" PHOTOMULTIPLYERS
IRON MAGNETIC SHIELDS
4" DIAMETER X 1" THICK COINCIDENCE
PLASTIC SCINTILLATOR
6" DIAMETER X 1" THICK ANTI-COINCIDENCE
PLASTIC SCINTILLATOR
12"

Fig. 2

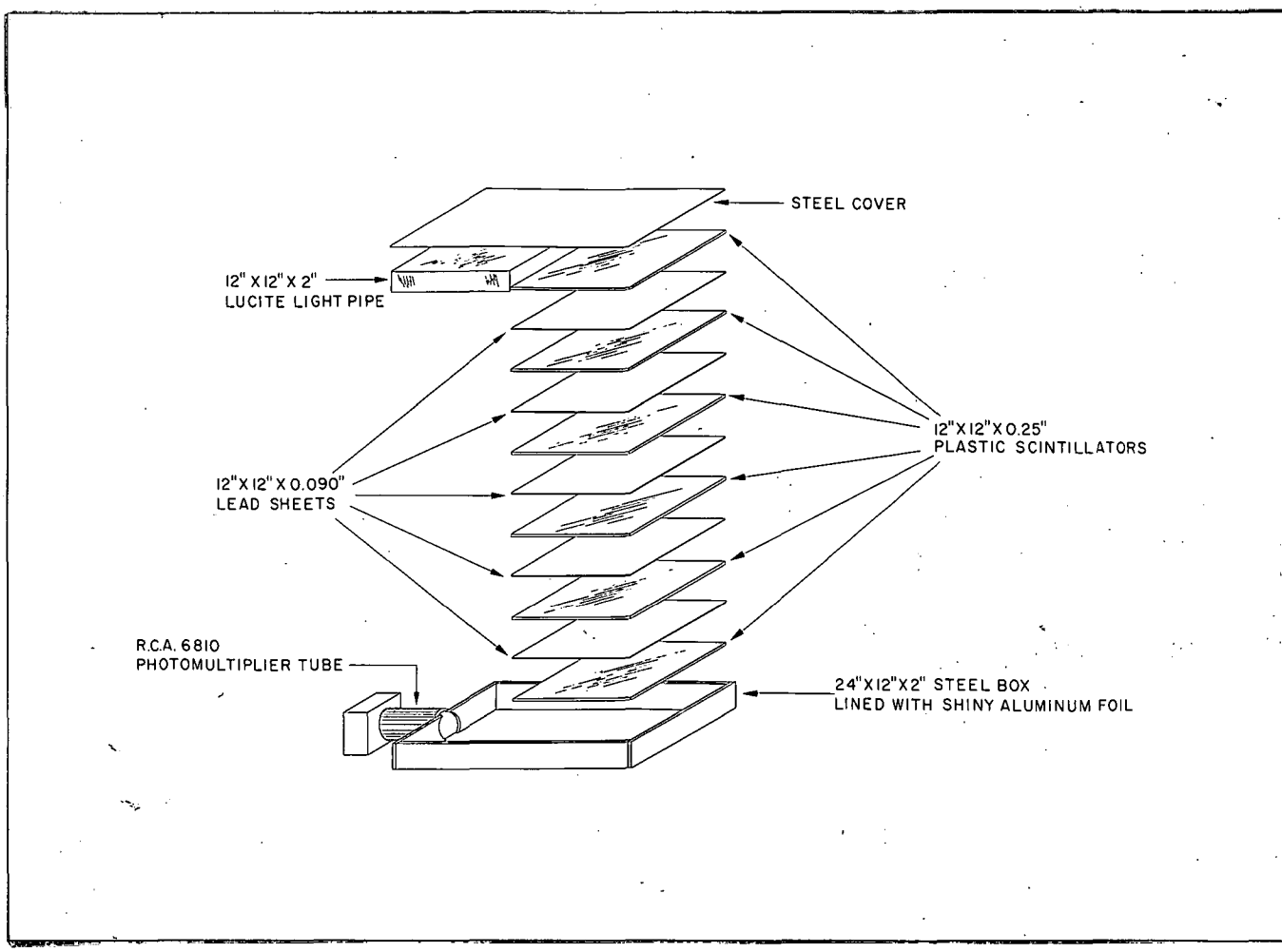
STEEL COVER
12" X 12" X 2"
LUCITE LIGHT PIPE
12"X12"X0.25"
PLASTIC SCINTILLATORS
12"X12"X0.090"
LEAD SHEETS
R.C.A. 6810
PHOTOMULTIPLIER TUBE
24"X12"X2" STEEL BOX
LINED WITH SHINY ALUMINUM FOIL

Fig. 3a

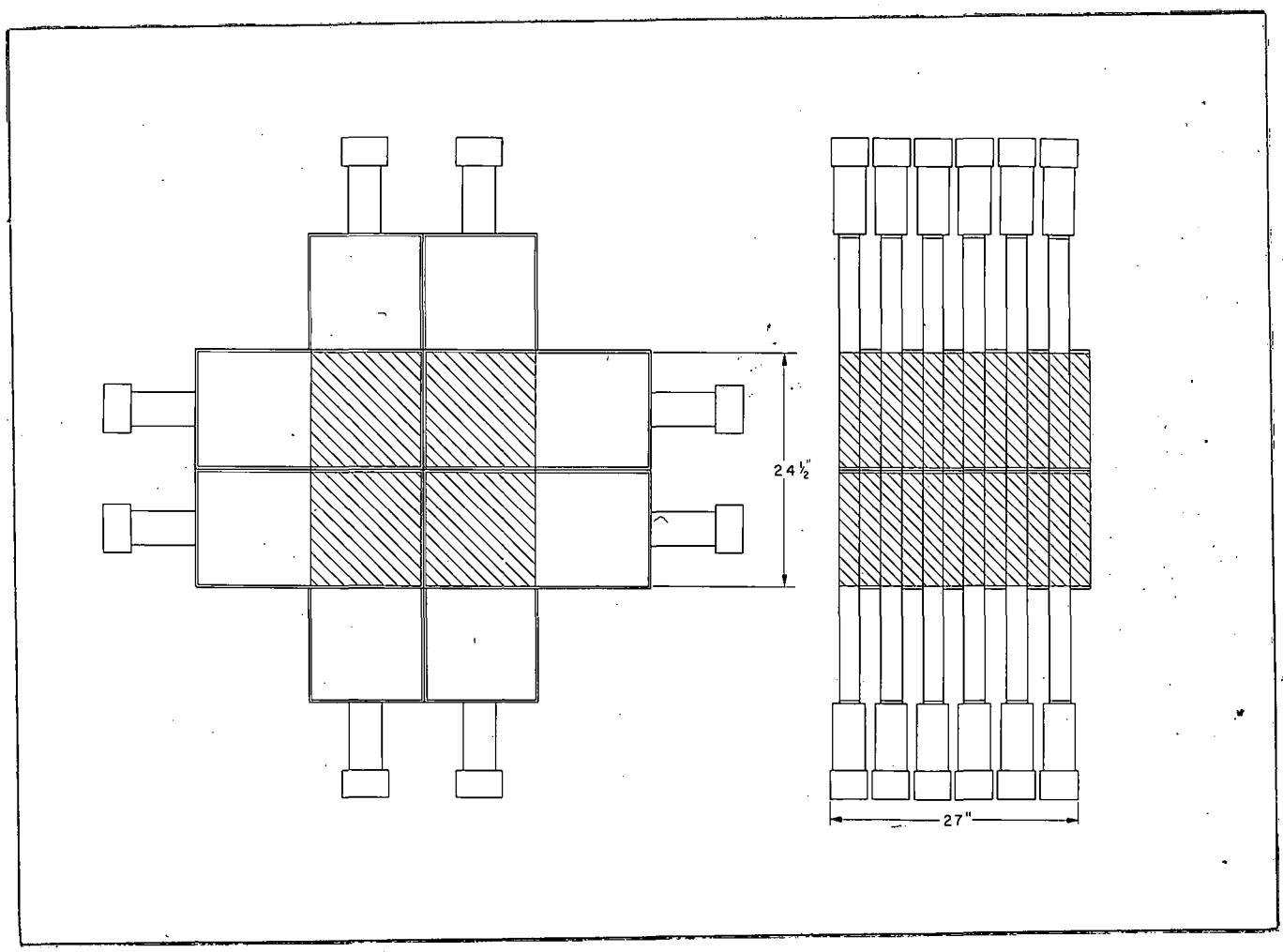

Fig. 3b

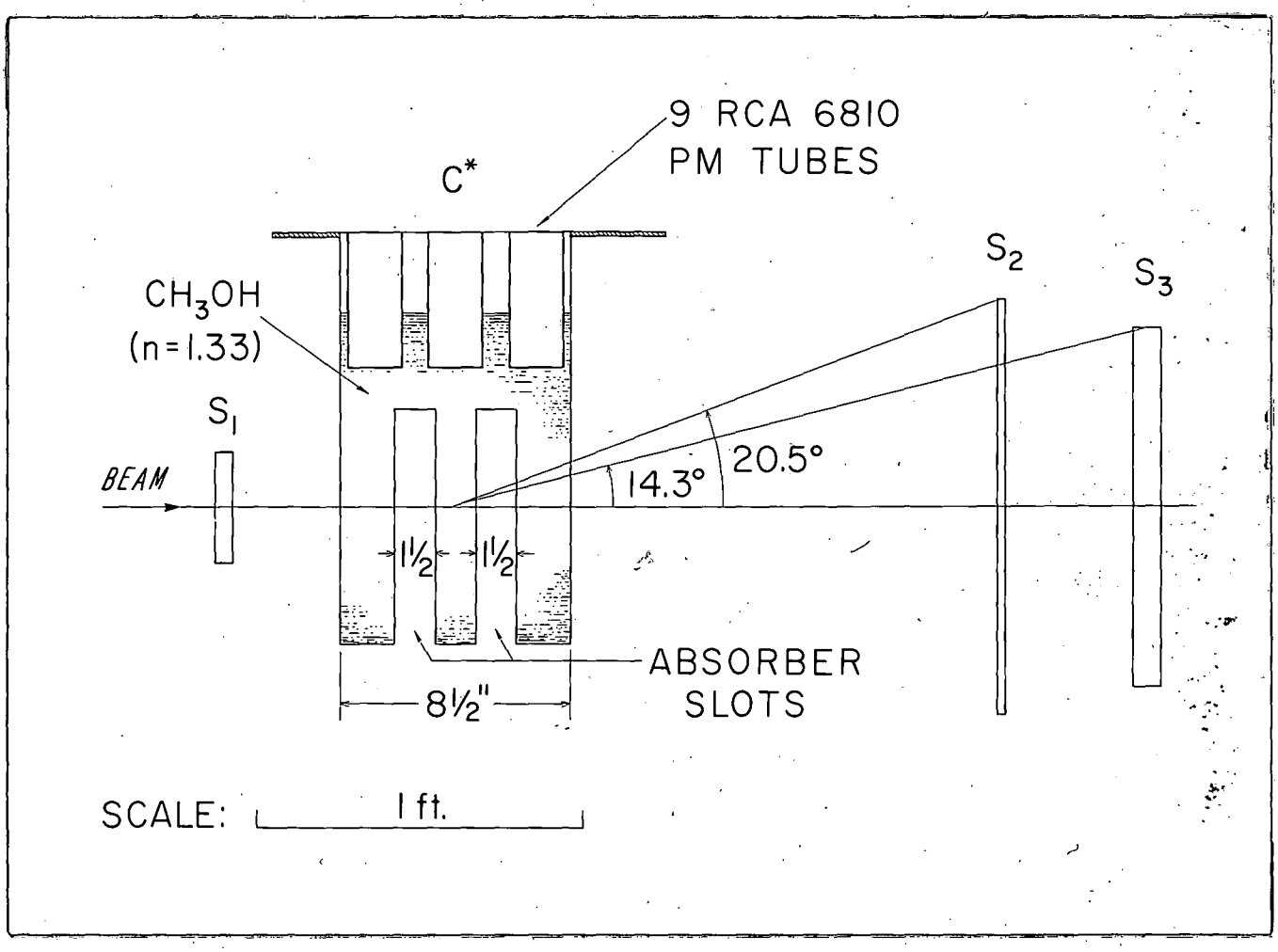
9 RCA 6810
PM TUBES
C*
S2
S3
CH3OH
(n=1.33)
S1
BEAM
14.3°
20.5°
1½
1½
ABSORBER
SLOTS
8½"
SCALE:
1 ft.

Fig. 4

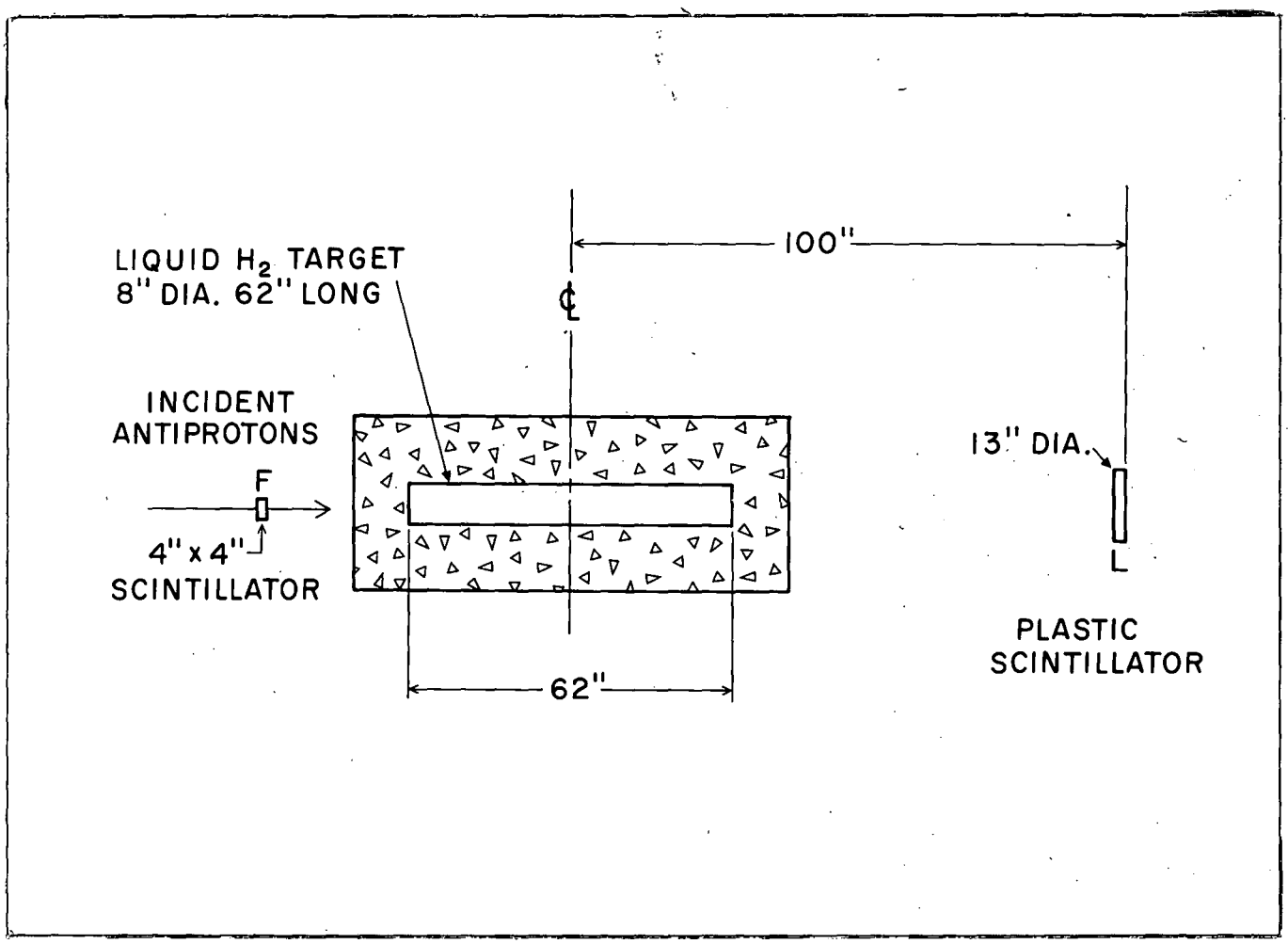
LIQUID H_2 TARGET
8" DIA. 62" LONG
INCIDENT
ANTIPROTONS
F
4" x 4"
SCINTILLATOR
100"
℄
13" DIA.
L
PLASTIC
SCINTILLATOR
62"

Fig. 5

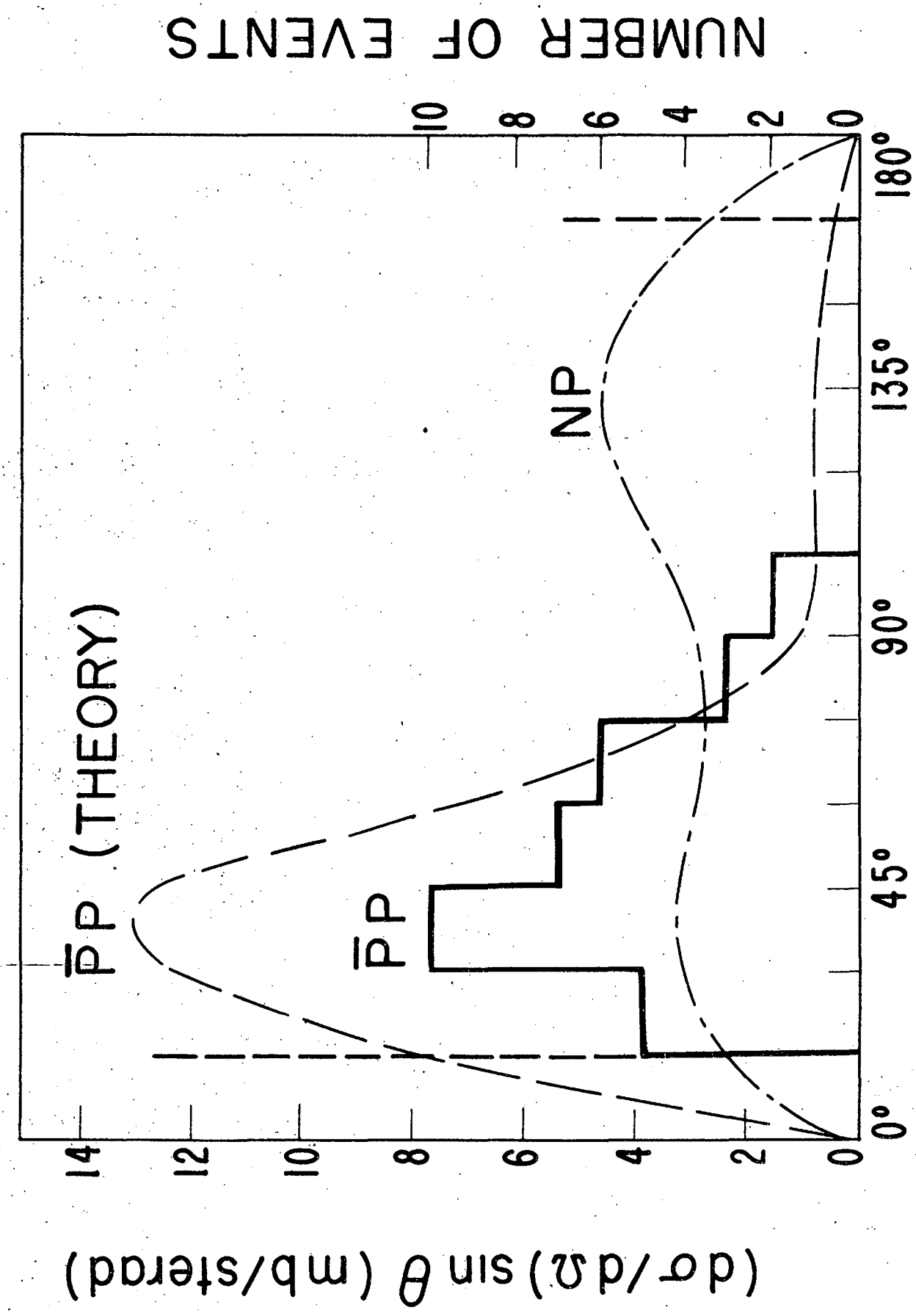
NUMBER OF EVENTS
10
8
6
4
2
0
180°
135°
90°
45°
0°
θ (c.m.)
NP
PP (THEORY)
PP
14
12
10
8
6
4
2
0
(dσ/dΩ) sin θ (mb/sterad)

Fig. 6

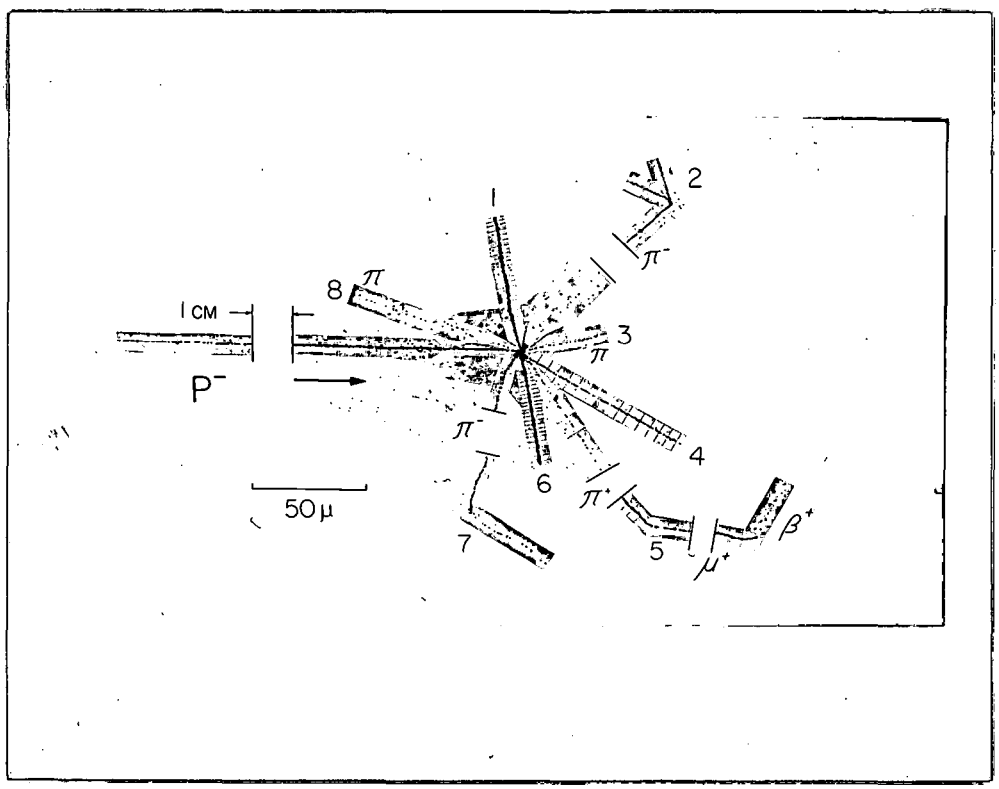

Fig. 7

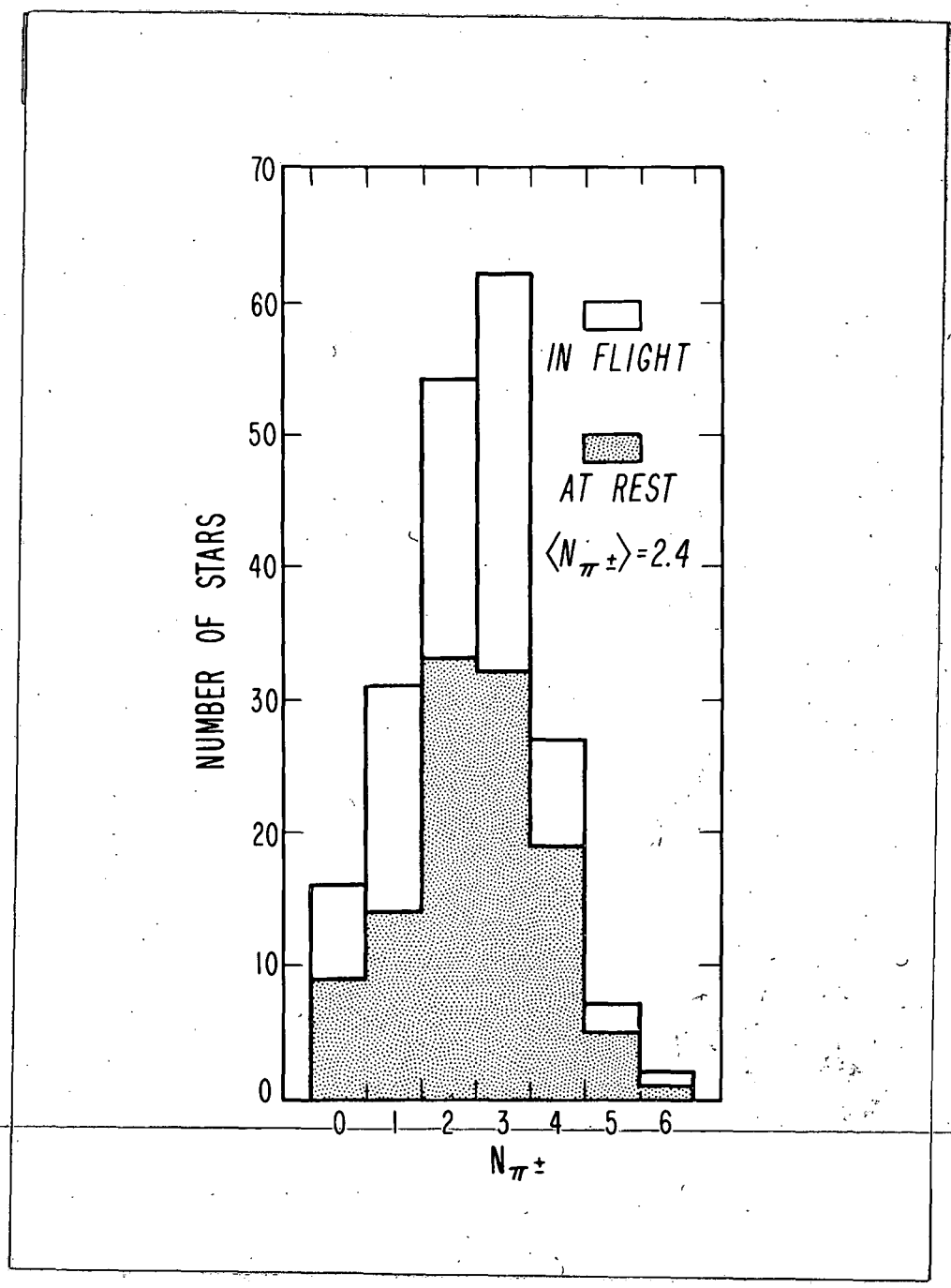
70
60
50
40
30
20
10
0
NUMBER OF STARS
IN FLIGHT
AT REST
⟨Nπ±⟩=2.4
0
1
2
3
4
5
6
Nπ±

Fig. 8

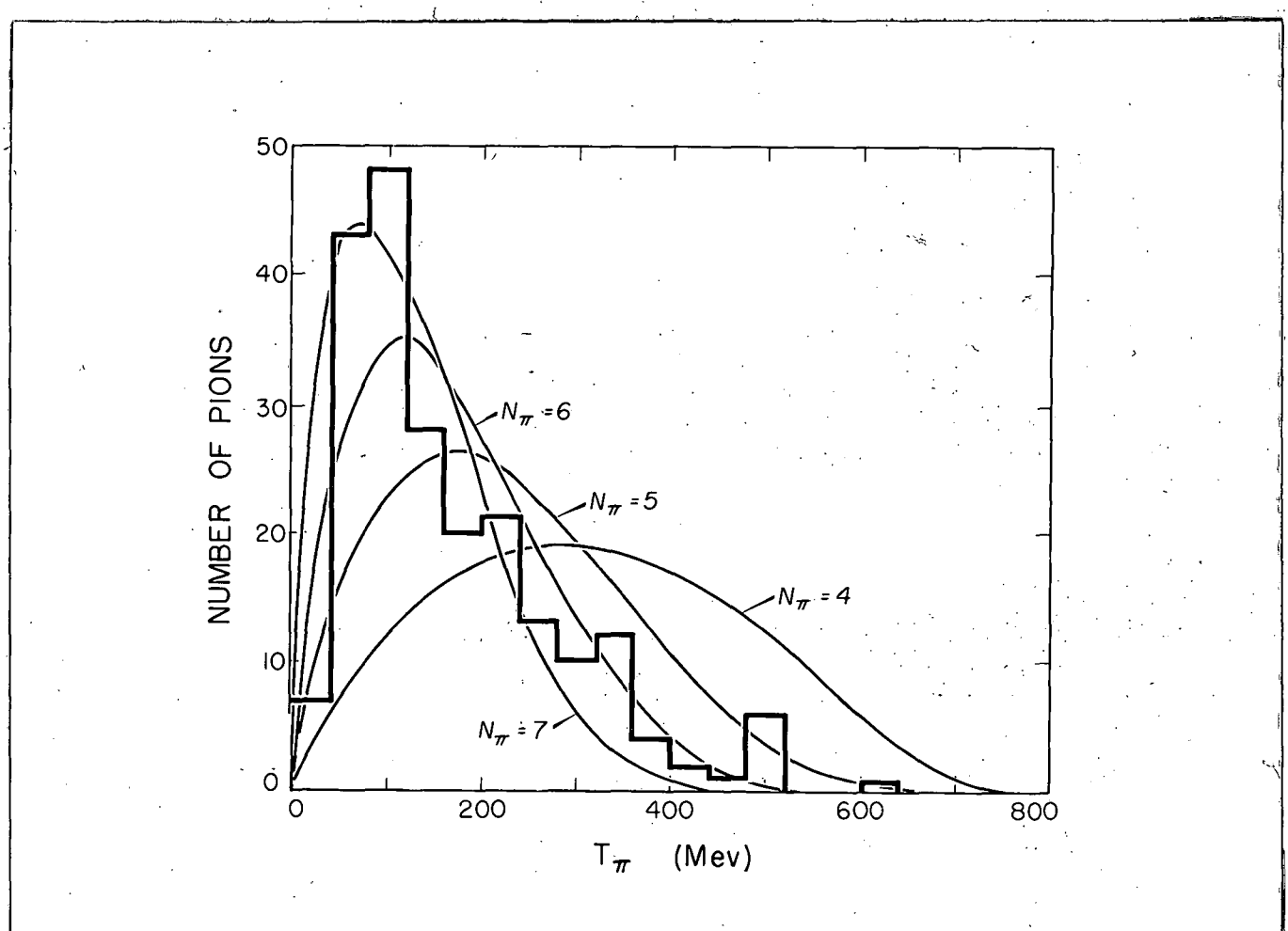
NUMBER OF PIONS
50
40
30
20
10
0
0
200
400
600
800
T_π (Mev)
$N_\pi = 6$
$N_\pi = 5$
$N_\pi = 4$
$N_\pi = 7$

Fig. 9

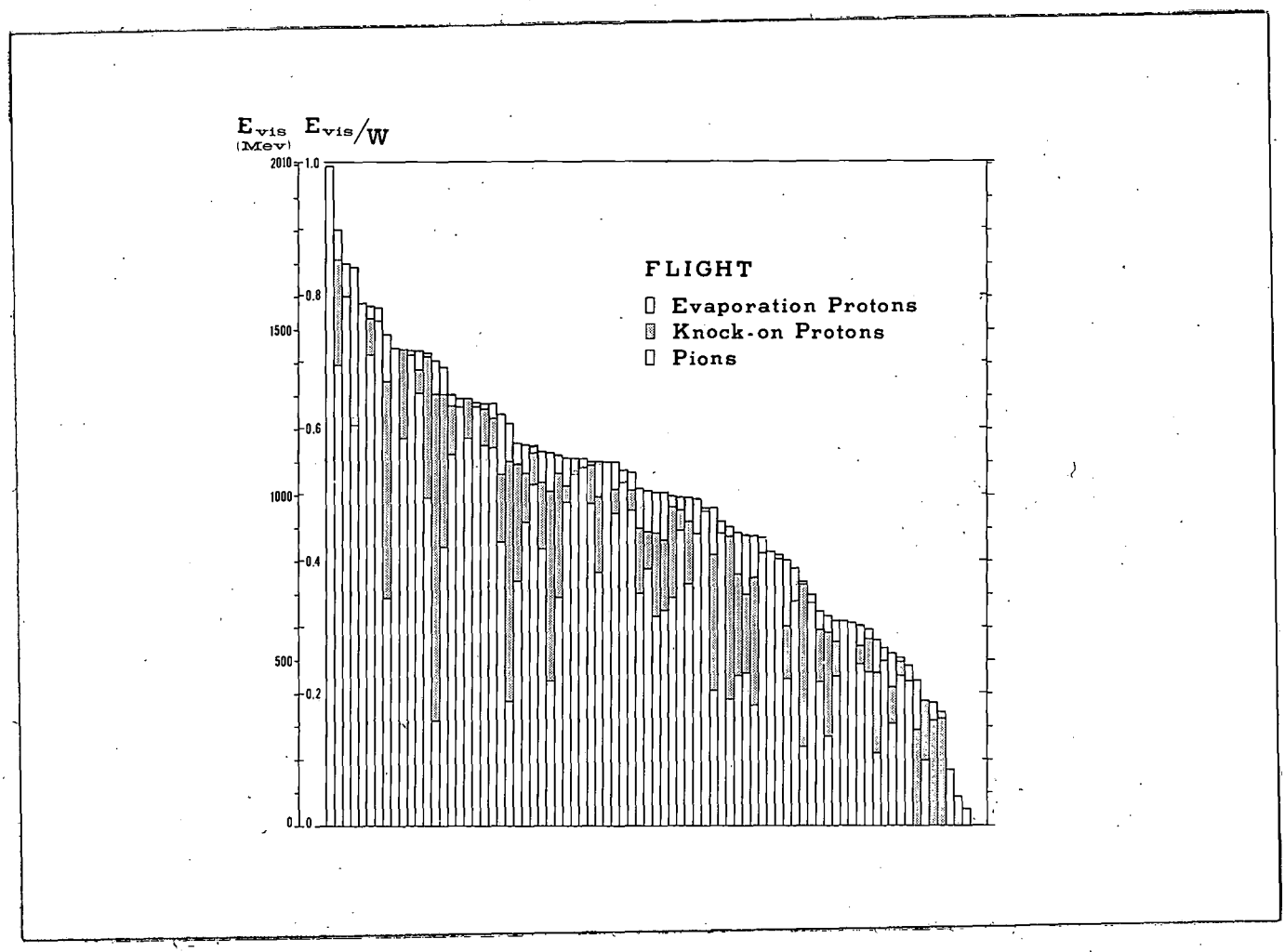
E_{vis} (Mev)
E_{vis}/W
2010
1500
1000
500
0
1.0
0.8
0.6
0.4
0.2
0
FLIGHT
Evaporation Protons
Knock-on Protons
Pions

Fig. 10a

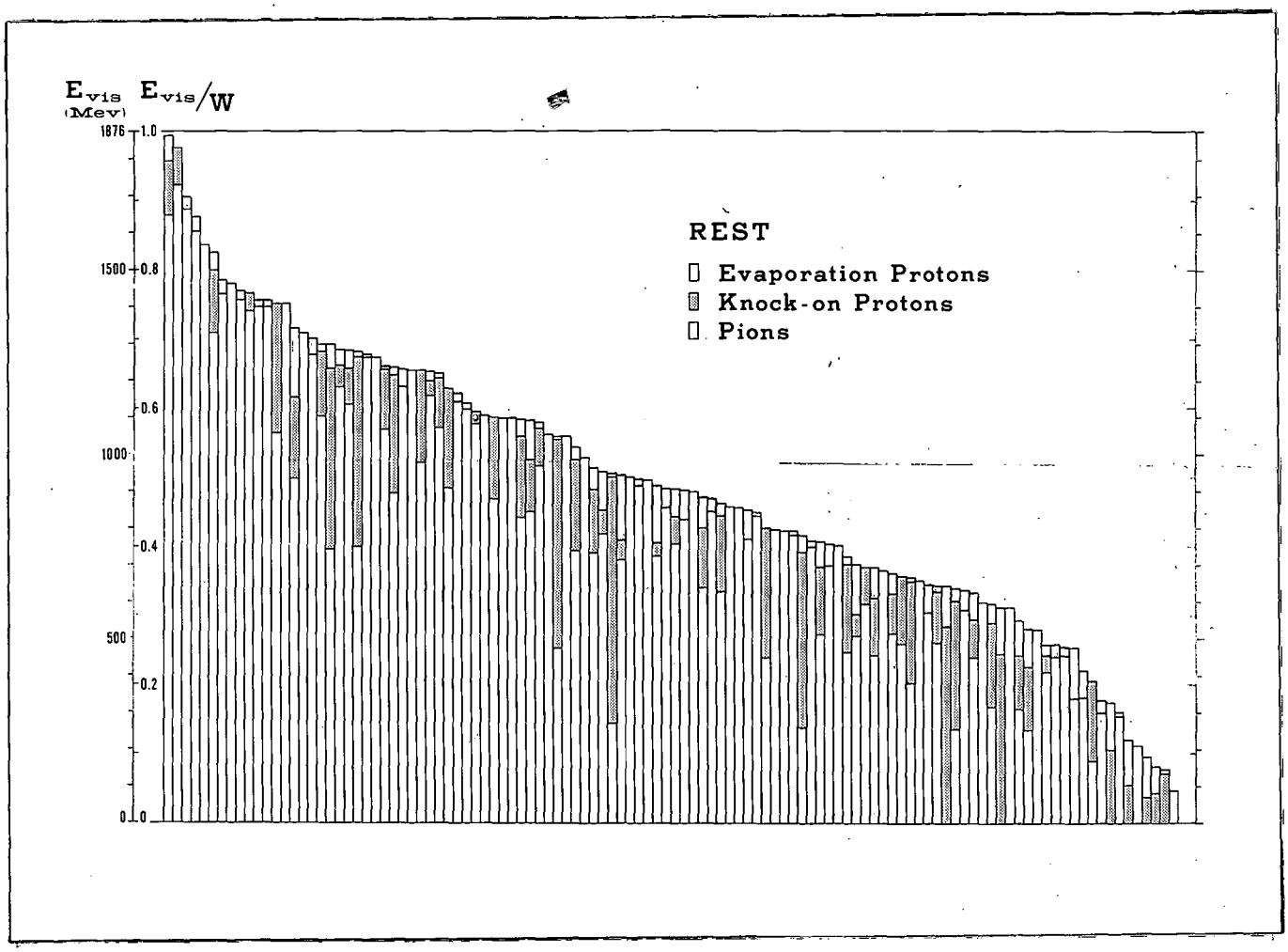
E_{vis} (Mev)
E_{vis}/W
1876
1500
1000
500
0
1.0
0.8
0.6
0.4
0.2
0
REST
Evaporation Protons
Knock-on Protons
Pions

Fig. 10b

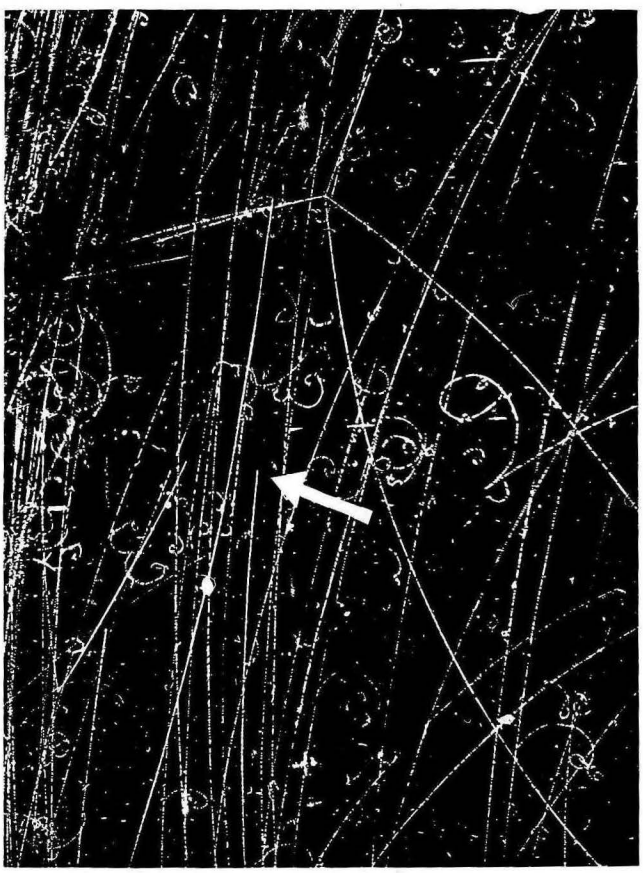

Fig. 11